DALTON
FULL PAPER

Hydrocarbyl derivatives of dppm- or dppa-bridged alkoxysilyl heterobimetallic Fe–Pd complexes and CO insertion reactions. Crystal structures of $[(OC)_3\{(MeO)_3Si\}Fe(\mu\text{-dppm})Pd(8\text{-mq})]$ (dppm = $Ph_2PCH_2PPh_2$), $[(OC)_3Fe\{\mu\text{-}Si(OMe)_2(OMe)\}(\mu\text{-dppa})PdCl]$ and $[(OC)_3Fe\{\mu\text{-}Si(OMe)_2(OMe)\}(\mu\text{-dppa})PdPh]$ (dppa = $Ph_2PNHPPh_2$)†

Pierre Braunstein,[a] Jérôme Durand,[a] Guido Kickelbick,[b] Michael Knorr,[a] Xavier Morise,[a] Raphael Pugin,[a] Antonio Tiripicchio[c] and Franco Ugozzoli[c]

[a] *Laboratoire de Chimie de Coordination, UMR 7513 du CNRS, Université Louis Pasteur, 4 rue Blaise Pascal, F-67070 Strasbourg Cedex, France. E-mail: braunst@chimie.u-strasbg.fr*
[b] *Institut für Anorganische Chemie, Technische Universität Wien, Getreidemarkt 9/153, A-1060 Wien, Austria*
[c] *Dipartimento di Chimica Generale ed Inorganica, Chimica Analitica, Chimica Fisica, Università di Parma, Centro di Studio per la Strutturistica Diffrattometrica del CNR, Parco Area delle Scienze 17A, I-43100 Parma, Italy*

Received 14th September 1999, Accepted 11th October 1999

The complexes $[(OC)_3Fe\{\mu\text{-}Si(OMe)_2(OMe)\}(\mu\text{-dppm})PdR]$ (R = alkyl, aryl) have been obtained either by treatment of $[(OC)_3Fe\{\mu\text{-}Si(OMe)_2(OMe)\}(\mu\text{-dppm})PdCl]$ **1a** with organolithium or Grignard reagents or, in the case where R = Me, by reaction of [PdCl(Me)(COD)] (COD = 1,5-cyclooctadiene) with the metallate $K[Fe\{Si(OMe)_3\}(CO)_3(dppm\text{-}P)]$ **2a**. When dppa was used as an assembling ligand, reaction of the hydrido complex *mer*-$[HFe\{Si(OMe)_3\}(CO)_3(dppa\text{-}P)]$ **7b** with [PdCl(Me)(COD)] or $[Pd(\eta^3\text{-allyl})(\mu\text{-Cl})]_2$ proceeded *via* elimination of methane or propene, respectively, to afford $[(OC)_3Fe\{\mu\text{-}Si(OMe)_2(OMe)\}(\mu\text{-dppa})PdCl]$ **1b** and not *via* HCl elimination which would have resulted in hydrocarbyl complexes. However, reaction of **7b** with [PdX(R)(TMEDA)] (X = Cl, R = Me; X = I, R = Ph; TMEDA = $Me_2NCH_2CH_2NMe_2$) afforded the hydrocarbyl complexes $[(OC)_3Fe\{\mu\text{-}Si(OMe)_2(OMe)\}(\mu\text{-dppa})PdMe]$ **3b** or $[(OC)_3Fe\{\mu\text{-}Si(OMe)_2(OMe)\}(\mu\text{-dppa})PdPh]$ **5b**. The latter and $[(OC)_3\{(MeO)_3Si\}Fe(\mu\text{-dppa})Pd(\eta^3\text{-allyl})]$ **8b** were obtained by reaction of the carbonylmetallate **2b** with [PdCl(Me)(COD)], [PdI(Ph)(TMEDA)] or $[Pd(\eta^3\text{-allyl})(\mu\text{-Cl})]_2$, respectively. The stabilizing but labile four-membered $\mu\text{-}\eta^2\text{-SiO}\rightarrow\text{Pd}$ bridging interaction facilitates CO insertion into the Pd–Me bond of **3a** or **3b** to afford the corresponding acetyl complexes. For comparison, $[(OC)_3\{(MeO)_3Si\}Fe(\mu\text{-dppm})Pd(8\text{-mq})]$ **6a** which contains a stable five-membered (*C*,*N*) chelate at Pd did not insert CO under similar conditions. The reaction of CO with the benzyl derivative $[(OC)_3Fe\{\mu\text{-}Si(OMe)_2(OMe)\}(\mu\text{-dppm})Pd(CH_2Ph)]$ **4a** was more complex since the resulting acyl $[(OC)_3Fe\{\mu\text{-}Si(OMe)_2(OMe)\}(\mu\text{-dppm})Pd\{C(O)CH_2Ph\}]$ **11a** rearranged into the μ-siloxycarbene complex $[(OC)_3Fe\{\mu\text{-}C(CH_2Ph)OSi(OMe)_3\}(\mu\text{-dppm})Pd(CO)]$ **12a**. Comparisons are made between complexes containing dppm or dppa and different R groups. The structures of complexes **1b**, **5b**·THF and **6a**·hexane have been determined by X-ray diffraction.

Introduction

Insertion reactions of small molecules into metal–carbon bonds represent elementary steps of considerable importance in organometallic chemistry and homogeneous catalysis.[1] Palladium complexes in particular have been widely studied from both a mechanistic and synthetic point of view.[2] These steps are involved in numerous stoichiometric and catalytic reactions, such as the Heck reaction,[3] carbonylation,[4] alternating polyketone synthesis (with the commercial developments of Carilon® by Shell and Ketonex® by BP Chemicals)[5] or olefin (co)-oligo- or -polymerization.[6] Whereas mononuclear palladium derivatives are attracting considerable attention, investigations on palladium-containing heterometallic complexes are scarce although they would provide interesting comparisons with the former. As part of our interest in the chemistry of heterobimetallic silyl complexes,[7] we have studied the insertion of small molecules such as CO, isocyanides or olefins into the palladium–alkyl bond of Fe–Pd complexes (Scheme 1) and of alkenes into the corresponding palladium–acyl bond, as well as alkynes into the platinum–acyl bond of related Fe–Pt complexes.[8]

These reactions proceed under mild conditions, *via* a mechanism which involves the hemilability of the alkoxysilyl ligand bound to the iron centre: opening of the $\text{SiO}\rightarrow\text{Pd}$ interaction releases a vacant coordination site at the palladium centre that becomes available to an incoming substrate (**A**) whereas, after

† *Supplementary data available*: rotatable 3-D crystal structure diagram in CHIME format. See http://www.rsc.org/suppdata/dt/1999/4175/

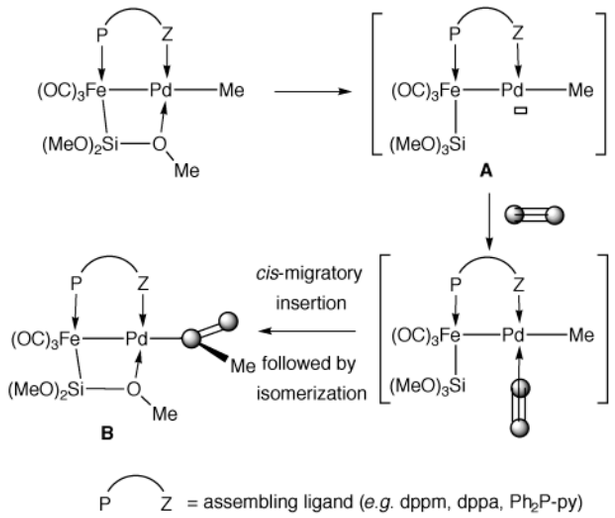

Scheme 1

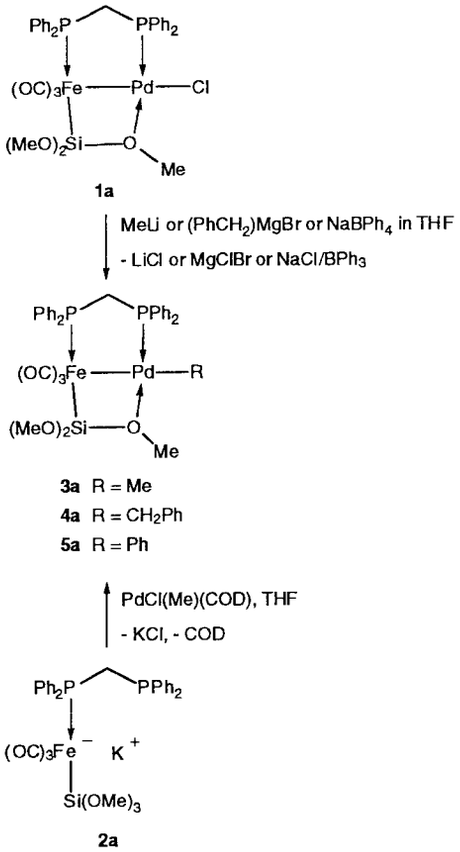

Scheme 2

insertion has occurred, the Fe–Si–O→Pd four membered ring is restored, thus stabilizing the product (**B**, Scheme 1). In this manner, polyketones and poly(iminomethylenes) have been prepared from CO/olefins and from isocyanides, respectively.[8a] A reaction mechanism also based on the hemilability of the $-Si(OMe)_3$ ligand has been proposed for the dehydrogenative coupling of tin hydrides catalyzed by heterobimetallic alkoxysilyl and siloxy Fe–Pd complexes, for which the predominant influence of the nature of the silyl ligand has been established.[9]

In order to develop further this insertion chemistry, a general access to "Fe–Pd–C" systems appeared desirable. We report here such investigations, with an emphasis on the use of the assembling ligands bis(diphenylphosphino)methane (dppm) and bis(diphenylphosphino)amine (dppa) in order to prevent (or retard) fragmentation during reaction into mononuclear complexes—a process well known to occur readily during reactivity studies with unsupported bimetallic complexes[10]—and to evaluate the influence of the assembling ligand on the synthesis and reactivity of the complexes. Some of the synthetic methods efficiently used in the case of Fe–Pd dppm complexes could not be applied to their dppa counterparts, owing to the relative acidity of the N–H function. Thus, an alternative approach had to be considered. In the numbering of the complexes, the letters **a** and **b** will refer to the dppm and dppa series, respectively.

Results and discussion

Dppm-bridged Fe–Pd–alkyl and –aryl complexes

The complexes $[(OC)_3Fe\{\mu\text{-}Si(OMe)_2(OMe)\}(\mu\text{-dppm})PdR]$ (R = alkyl, aryl) have been prepared either by treatment of the known chloro complex $[(OC)_3Fe\{\mu\text{-}Si(OMe)_2(OMe)\}(\mu\text{-dppm})PdCl]$ **1a**[11] with organolithium or Grignard reagents or in the case where R = Me by reaction of [PdCl(Me)(COD)] (COD = 1,5-cyclooctadiene) with the metallate $K[Fe\{Si(OMe)_3\}(CO)_3(dppm\text{-}P)]$ **2a** (Scheme 2).

Thus, reaction of **1a** with MeLi, in THF at 253 K, led to the bright yellow methyl complex $[(OC)_3Fe\{\mu\text{-}Si(OMe)_2(OMe)\}(\mu\text{-dppm})PdMe]$ **3a** which has a moderate solubility in Et_2O but is very soluble in THF, CH_2Cl_2 or toluene. The yield of this reaction did not exceed 25% and we assume that this is in part due to competing side-reactions, such as nucleophilic attack of MeLi on the iron carbonyl ligands. In order to circumvent this problem, we reacted **2a** with [PdCl(Me)(COD)] (Scheme 2). IR monitoring of this reaction revealed the rapid and almost quantitative formation of **3a** within 10 min. After workup, the latter was obtained in *ca.* 75% yield. Note that contrary to the very stable Pt ethyl derivative $[(OC)_3Fe\{\mu\text{-}Si(OMe)_2(OMe)\}(\mu\text{-dppm})PtEt]$,[12] the Fe–Pd–Et analogue of **3a** could not be obtained by treatment of **1a** with EtMgBr. Instead, rapid decomposition to unidentified products and black insoluble materials (Pd^0) was observed, probably owing to facile β-elimination. However when benzyl magnesium chloride was employed (THF, 253 K), yellow-orange $[(OC)_3Fe\{\mu\text{-}Si(OMe)_2(OMe)\}(\mu\text{-dppm})Pd(CH_2Ph)]$ **4a** was obtained in 68% yield. The heterobimetallic complexes **3a** and **4a** are stable and may be kept as solids in the air or in solution under nitrogen for several hours without significant decomposition. This behaviour contrasts with that of numerous mononuclar Pd–alkyl complexes which tend to rapidly decompose under similar conditions. When **3a** was treated with small amounts of MeOH or water, no elimination of methane was observed. Slow cleavage of the Pd–alkyl bond was however observed after several days in $CDCl_3$ on exposure to light, with formation of **1a**. Surprisingly, attempts to prepare the aryl complex $[(OC)_3Fe\{\mu\text{-}Si(OMe)_2(OMe)\}(\mu\text{-dppm})PdPh]$ **5a** by treatment of **1a** with PhLi or PhMgX were unsuccessful. However, slow formation of **5a** was observed ($^{31}P\{^1H\}$ NMR monitoring and comparison with an authentic sample, see below) when **1a** was reacted with $NaBPh_4$ in THF but decomposition products appeared before completion of the reaction. Selected spectroscopic data for the new complexes are given in Table 1.

The presence of a $\mu\text{-}\eta^2\text{-}Si\text{–}O$ interaction with the Pd centre in **3a** was indicated by the very broad ^1H NMR resonance at δ 3.91 for the nine methoxy protons in C_6D_6 at 298 K. Although this signal sharpens when raising the temperature, it remains broad even at 333 K, indicating a slow exchange of the methoxy groups on the NMR time scale. The singlet at δ 0.82 was assigned to the Pd-methyl protons and the triplet at δ 3.49 to the dppm methylenic protons. The resonance of the methoxy

Table 1 Selected $^{31}P\{^1H\}$ NMR (ppm, Hz) and IR data (cm^{-1})

Complex	δP_{Fe}	δP^a	$^{2+3}J(PP)$	$\nu(CO)$
2a[b]	74.2	−23.8	79	1919w, 1824vs[c]
2b[b]	123.9	27.6	31	1928w, 1840vs[c]
3a	63.5	42.2	51[d]	1956m, 1892s, 1862vs[c]
3b	113.9	84.0	53[e]	1963m, 1899s, 1877s[c]
4a	60.7	36.3	53[e]	1955s, 1893s, 1864vs[c]
5a	61.7	33.9	51[f]	1959s, 1894s, 1866vs[c]
5b	114.5	79.3	52[f]	1965s, 1925m, 1893s[c]
6a	63.0	32.7	72[g]	1945s, 1870vs, 1838vs[c]
7a	52.1	−24.7	104[f]	2042w, 1982s, 1975vs[h]
7b	103.1	33.0	58[d]	2054w, 1990sh, 1981vs[i]
8a	67.1	27.7	106[g]	1956s, 1889m, 1861vs[j]
8b	119.1	79.4	116[f]	1960m, 1885s, 1874s[c]
9	113.9	101.1	61[d]	2006s, 1964s, 1925w[c]
10a	65.2	26.7	55[e]	1958s, 1893vs, 1864vs, 1678m[c]
10b	115.5	69.6	59[e]	1965s, 1901vs, 1878vs, 1676m[c]
11a	63.4	25.5	56[e]	1958m, 1895s, 1865vs, 1678m, br[c]
16a	66.0	18.7	89[e,k]	2176m, 1949m, 1877s, 1850vs, 1690m[c]

[a] P atom of the dppm or dppa ligand coordinated to Pd except in **2a**,**b** and **7a**,**b** (dangling); [b] as the $[HNEt_3]^+$ salt; [c] in CH_2Cl_2; [d] in CH_2Cl_2/C_6D_6; [e] in $CDCl_3$; [f] in acetone-d_6; [g] in CH_2Cl_2/acetone-d_6; [h] in Et_2O; [i] in hexane; [j] in THF; [k] recorded at 243 K.

protons began to split below the coalescence temperature (*ca.* 273 K in $CDCl_3$) and at 233 K, two distinct singlets were observed at δ 3.77 and 3.68 in a 2:1 ratio. The narrow singlet at δ 3.76 for the $Si(OMe)_3$ resonance of the benzyl derivative **4a** in $CDCl_3$ at 298 K indicates a fast exchange regime. A significant broadening of the $Si(OMe)_3$ resonance was also observed in the $^{13}C\{^1H\}$ NMR spectrum of **3a**, where the signal appeared at δ 50.7. In contrast, the singlet assigned to the Pd-bound methyl group at δ 15.7, the doublet of doublets of the dppm-methylene carbon at δ 47.3, and the two doublets of the iron carbonyls at δ 215.9 and 213.4 (in a 2:1 ratio) were all well resolved. The methoxy $^{13}C\{^1H\}$ resonance of the benzyl derivative **4a** appeared however as a narrow singlet at δ 50.8. As expected, the $^{31}P\{^1H\}$ NMR resonances for **3a** and **4a** show an AX pattern for the phosphorus nuclei bound to Fe (δ 63.5 and 60.7) and Pd (δ 42.2 and 36.3), respectively. They display a typical $^{2+3}J(PP)$ coupling of *ca.* 52 Hz generally observed in Fe–Pd bimetallics showing this type of μ-η^2-Si–O interaction[7,12] (see below).

An interesting comparison between the competing coordination properties of an oxygen atom and a nitrogen donor was provided by the reaction of **2a** with the dimeric, halide-bridged cyclopalladated complex $[Pd(8\text{-mq})(\mu\text{-Cl})]_2$ which contains a chelating 8-methylquinoline ligand (8-mq). Addition of 2 equivalents of **2a** to a slurry of $[Pd(8\text{-mq})(\mu\text{-Cl})]_2$ in THF led to rapid formation of the very stable, bright yellow compound $[(OC)_3\{(MeO)_3Si\}\overline{Fe(\mu\text{-dppm})Pd(8\text{-mq})}]$ **6a** in 92% yield (eqn. (1)).

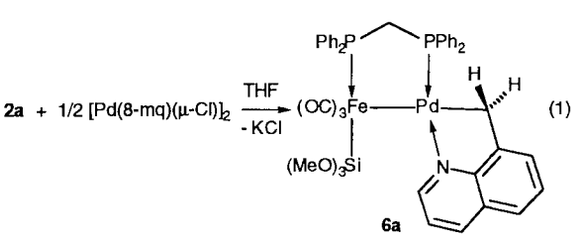

The $^{31}P\{^1H\}$ NMR spectrum of **6a** differed markedly from those of the methyl and benzyl derivatives **3a** and **4a** ($^{2+3}J(PP) = 51$ and 53 Hz respectively) by its large $^{2+3}J(PP)$ coupling of 72 Hz. Coordination of the nitrogen was evidenced in the ^1H NMR spectrum in $CDCl_3$ by a broadened triplet at δ 9.96 for the *ortho* proton of the pyridine ring, which shows a coupling of 3.9 Hz with the P nucleus on Pd. The CH_2 protons of the dppm ligand appear as a doublet of doublets at δ 3.83 and the equivalent CH_2 protons of the quinoline ring give rise

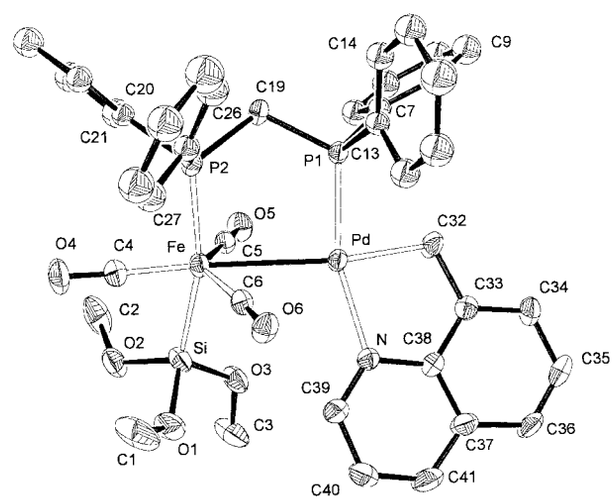

Fig. 1 ORTEP[34] view of the structure of the complex **6a** in **6a**·hexane together with the atomic numbering scheme. The ellipsoids for the atoms are drawn at the 30% probability level.

to a doublet at δ 2.93 owing to a *cis*-coupling of $^3J(PH) = 4.2$ Hz. The sharp $Si(OMe)_3$ resonance at δ 3.55 did not broaden upon cooling to 253 K, in agreement with the absence of any significant SiO→Pd interaction in solution. Formation of a five-membered chelate ring $\overline{Pd–C–C–C–N}$ is obviously prefered here over that of a four-membred ring $\overline{Fe–Si–O\rightarrow Pd}$ although we have noted previously that the latter interaction is able to displace a pyridine-type ligand.[12b] The relatively low values found for the $\nu(CO)$ vibrations at 1945, 1870 and 1838 cm^{-1} in CH_2Cl_2 reflect the donor properties of the *C*,*N* chelate and are indicative of semi-bridging carbonyl interaction(s) with the Pd centre. The structure of **6a**·hexane has been determined by X-ray diffraction. A view of the structure is depicted in Fig. 1 and selected interatomic distances and angles are given in Table 2.

Both the geometries at the metal centres, square planar at Pd and octahedral at Fe, are severely distorted. The coordination around the Pd atom involves the Fe atom, the P(1) atom from the dppm bridging ligand and, as expected, the N and C(32) atoms from the metallated 8-methylquinoline which acts as a chelating ligand. Both the bite angle N–Pd–C(32) of the chelate, 81.8(5)°, and the P(1)–Pd–C(32) angle, 82.8(5)°, are very acute, whereas the Fe–Pd–N angle is very large, 105.5(3)°. The quinoline moiety and the chelate ring are perfectly coplanar.

Table 2 Selected bond lengths (Å) and angles (°) for [(OC)$_3${(MeO)$_3$Si}-Fe(μ-dppm)Pd(8-mq)] **6a**·hexane

Pd–Fe	2.850(2)	Pd–P(1)	2.227(4)
Pd–N	2.15(1)	Pd–C(32)	2.061(14)
Fe–P(2)	2.206(4)	Fe–Si	2.279(4)
Fe–C(4)	1.735(15)	Fe–C(5)	1.763(16)
Fe–C(6)	1.767(15)	P(1)–C(19)	1.83(1)
P(2)–C(19)	1.82(1)	Si–O(1)	1.66(1)
Si–O(2)	1.67(1)	Si–O(3)	1.65(1)
O(1)–C(1)	1.33(2)	O(2)–C(2)	1.43(2)
O(3)–C(3)	1.40(2)	O(4)–C(4)	1.16(2)
O(5)–C(5)	1.19(2)	O(6)–C(6)	1.17(2)
N–C(38)	1.39(2)	N–C(39)	1.28(2)
N–Pd–C(32)	81.8(5)	P(1)–Pd–C(32)	82.8(5)
P(1)–Pd–N	161.0(3)	Fe–Pd–C(32)	167.9(4)
Fe–Pd–N	105.5(3)	Fe–Pd–P(1)	91.6(1)
Pd–Fe–C(6)	62.5(5)	Pd–Fe–C(5)	71.3(5)
Pd–Fe–C(4)	172.4(5)	Pd–Fe–Si	101.8(1)
Pd–Fe–P(2)	92.3(1)	C(5)–Fe–C(6)	132.2(7)
C(4)–Fe–C(6)	109.9(7)	C(4)–Fe–C(5)	116.2(7)
Si–Fe–C(6)	93.4(5)	Si–Fe–C(5)	83.8(5)
Si–Fe–C(4)	78.5(5)	P(2)–Fe–C(6)	98.4(5)
P(2)–Fe–C(5)	95.3(4)	P(2)–Fe–C(4)	88.4(5)
P(2)–Fe–Si	164.8(2)	Pd–P(1)–C(19)	116.2(4)
Fe–P(2)–C(19)	112.5(5)	Pd–N–C(39)	129.4(11)
C(38)–N–C(39)	118.3(12)	Fe–C(4)–O(4)	176.6(14)
Fe–C(5)–O(5)	178.3(13)	Fe–C(6)–O(6)	172.5(13)
Pd–C(6)–O(6)	107.2(9)	Pd–C(6)–Fe	79.9(5)
Pd–C(32)–C(33)	109.6(9)		

The Fe–Pd bond length, 2.850(2) Å, is significantly longer than in related structures containing a (OC)$_3$(Si)Fe(P)–PdP fragment (*cf.* 2.582(1) Å in **1a**).[8b,11,13] There are no bonding interactions between the Pd atom and the Si(OMe)$_3$ group. The short Pd···C(6) contact, 2.569(14) Å, more than the value of the Pd–C(6)–O(6) angle, 107.2(9)°, may be indicative of a semi-bridging character of a carbonyl ligand.

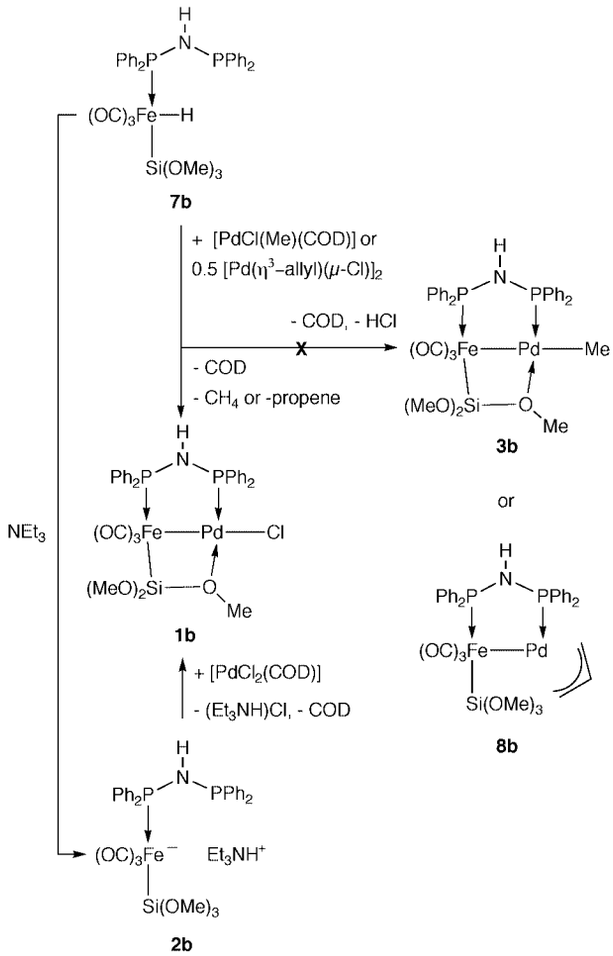

Scheme 3

Dppa-bridged Fe–Pd–alkyl and –aryl complexes

For comparative purposes, we set out to prepare dppa-bridged Fe–Pd–alkyl and –aryl alkoxysilyl complexes by using the methodology described above for their dppm analogues. This required the use of the chloro complex [(OC)$_3$Fe{μ-Si(OMe)$_2$(OMe)}(μ-dppa)PdCl] **1b** as precursor. This complex has been previously prepared from [PdCl$_2$(COD)] and the carbonylmetallate [HNEt$_3$][Fe{Si(OMe)$_3$}(CO)$_3$-(dppa-*P*)] **2b** (Scheme 3),[14] itself obtained by deprotonation of *mer*-[HFe{Si(OMe)$_3$}(CO)$_3$(dppa-*P*)] **7b** with NEt$_3$. Use of stronger bases, such as KH, led to concomitant deprotonation of the amine function of the dppa ligand. Note that **7b**, which is a highly air- and moisture-sensitive oil, tends to decompose upon loss of CO to give the hydrido, chelated complex [HFe{Si(OMe)$_3$}(CO)$_2$(dppa-*P,P′*)]. This behaviour contrasts with that of its dppm analogue for which reductive elimination of HSi(OMe)$_3$ and formation of [Fe(CO)$_3$(dppm-*P,P′*)] were observed instead.

Direct treatment of the hydrido complex **7b** with [PdCl(Me)-(COD)] or [Pd(η^3-allyl)(μ-Cl)]$_2$ selectively led to **1b** in higher yields than the anionic route (Scheme 3). These reactions proceed *via* clean elimination of methane or propene, respectively, and avoid previous deprotonation of **7b**. It is interesting that an alternative reaction pathway consisting of HCl elimination and formation of the hydrocarbyl complexes **3b** or **8b** was not observed (Scheme 3). The alkoxysilyl ligand in **1b** adopts a μ-η^2-Si–O coordination mode as in **1a** and exhibits a hemilabile behaviour at room temperature, as shown in the ^{1}H NMR spectrum by the broad signal at δ 3.70 due to the equivalence of the three methoxy groups. This resonance shifted slightly upfield and broadened upon progressive cooling until coalescence was reached ($T_c = 262$ K, $\Delta G^{\ddagger} = 54.15 \pm 0.7$ kJ mol^{-1}).[15] Below coalescence temperature, two signals were observed at δ 3.62 and 3.49 in a 2:1 ratio. This contrasts with **1a** for which coalescence was still not reached at 178 K. Comparison between the ^{31}P{^{1}H} NMR and IR data of **1a** and **1b** shows smaller downfield shifts between coordinated and free phosphines for the dppa than for the dppm derivatives and ν(CO) vibrations at higher wavenumbers in **1b** than in **1a** (Table 3). These two features are explained by dppa being a weaker electron donor than dppm. Interestingly, the ν(Pd–Cl) vibration was observed at 290 cm^{-1} for **1b** instead of 270 cm^{-1} for **1a** whereas [Pd$_2$Cl$_2$-(μ-dppm)$_2$][16] and [Pd$_2$Cl$_2$(μ-dppa)$_2$][17] have similar ν(Pd–Cl) vibrations (249 and 255 cm^{-1} respectively).

The structure of **1b** was confirmed by an X-ray diffraction study. A view of the structure is depicted in Fig. 2 and selected interatomic distances and angles are given in Table 4. The Fe–Pd bond distance, 2.554(4) Å, is slightly shorter than in the dppm analogue **1a**, 2.582(1) Å.[11] The square-planar geometry about the Pd centre is achieved by coordination of the O(4) atom of the silyl moiety. The Pd–O(4) bond distance of 2.178(19) Å is longer than in **1a**, 2.100(4) Å,[11] but close to that found in [(OC)$_3$Fe{μ-Si(OMe)$_2$(OMe)}(μ-dppm)Pd(SnPh$_3$)], 2.165(2) Å.[13] The Si–O(4) bond, 1.66(2) Å, is only slightly elongated, compared to the other two Si–O bonds in the molecule, 1.595(15) and 1.63(3) Å. This is a consequence of the O(4)→Pd interaction. The Pd–Cl bond, 2.385(8) Å, is longer than in **1a**, 2.303(2) Å.[11] The Fe centre has a distorted octahedral environment with a *trans*-P–Fe–Si arrangement, P(1)–Fe–Si 174.0(2)°. The distortion of the geometry at the iron centre is reflected in the Si–Fe–Pd angle of 75.8(3)°, that is more acute than in related complexes in which there is no SiO bridge, such as **6a**, 101.8(1)° or [(OC)$_3${(MeO)$_3$Si}Fe(μ-dppm)Pd(η^3-allyl)] **8a**, 93.38(4)°.[13]

Table 3 Comparison between selected $^{31}P\{^1H\}$ NMR (in CH_2Cl_2, ppm, Hz) and IR data (in CH_2Cl_2, cm^{-1}) for **1a** and **1b**

Complex	δP_{Fe}	$\Delta\delta$[a]	δP_{Pd}	$\Delta\delta$[a]	^{2+3}J(PP)	ν(CO)
1a	48.0 (d)	*+70.0*	34.9 (d)	*+56.9*	55	1995s, 1940vs, 1923s
1b	100.8 (d)	*+58.8*	85.8 (d)	*+43.8*	51	2002s, 1946vs, 1935sh

[a] Coordination chemical shift ($\delta_{complex} - \delta_{free\ ligand}$); dppm = −22 and dppa = 42 ppm.

Table 4 Selected bond lengths (Å) and angles (°) for [$(OC)_3$-Fe{μ-Si$(OMe)_2$(OMe)}(μ-dppa)PdCl] **1b**

Pd–Fe	2.554(4)	Pd–P(2)	2.188(7)
Pd–Cl	2.385(8)	Pd–C(3)	2.52(3)
Pd–O(4)	2.178(19)	Fe–Si	2.291(9)
Fe–P(1)	2.210(7)	Fe–C(2)	1.77(3)
Fe–C(1)	1.768(17)	P(1)–N	1.69(2)
Fe–C(3)	1.78(2)	P(1)–C(10)	1.820(14)
P(1)–C(4)	1.84(2)	P(2)–C(16)	1.81(3)
P(2)–C(22)	1.806(12)	P(2)–N	1.68(2)
Si–O(4)	1.66(2)	Si–O(5)	1.595(15)
Si–O(6)	1.63(3)	O(1)–C(1)	1.15(2)
O(2)–C(2)	1.13(4)	O(3)–C(3)	1.16(2)
O(4)–C(28)	1.44(4)	O(5)–C(29)	1.33(3)
O(6)–C(30)	1.32(7)		
Fe–Pd–C(l)	173.7(2)	Fe–Pd–O(4)	80.7(5)
P(2)–Pd–Cl	94.4(2)	P(2)–Pd–O(4)	172.5(3)
Cl–Pd–O(4)	93.1(6)	Pd–Fe–P(1)	98.2(2)
Fe–Pd–P(2)	91.8(2)	Pd–Fe–C(1)	83.6(10)
Pd–Fe–Si	75.8(3)	Pd–Fe–C(3)	68.4(10)
Pd–Fe–C(2)	163.0(9)	P(1)–Fe–C(1)	92.3(5)
P(1)–Fe–Si	174.0(2)	P(1)–Fe–C(3)	91.0(5)
P(1)–Fe–C(2)	97.9(5)	Si–Fe–C(2)	88.1(5)
Si–Fe–C(1)	86.2(6)	C(1)–Fe–C(2)	101.1(8)
Si–Fe–C(3)	87.6(5)	C(2)–Fe–C(3)	106.0(11)
C(1)–Fe–C(3)	152.0(6)	Pd–P(2)–N	115.6(4)
Fe–P(1)–N	109.7(4)	Pd–O(4)–Si	101.3(6)
Fe–Si–O(4)	101.2(5)	Si–O(4)–C(28)	127.3(17)
Pd–O(4)–C(28)	131.1(8)	P(1)–N–P(2)	121.8(12)

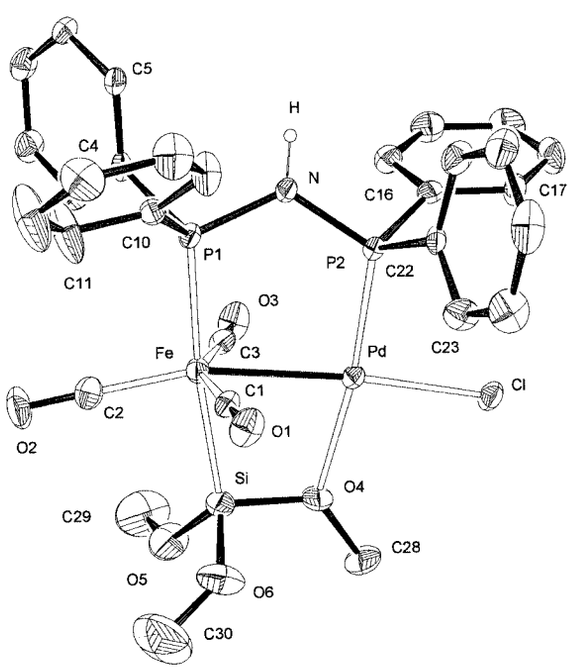

Fig. 2 ORTEP view of the structure of the complex **1b** together with the atomic numbering scheme. The ellipsoids for the atoms are drawn at the 30% probability level.

Treatment of **1b** with alkylating reagents (RLi, RMgX, SnR_4, *etc.*) did not afford the desired Pd–alkyl derivatives (Scheme 4). Instead, either decomposition was observed or **1b** was recovered. The former may result from side reactions involving the relatively acidic NH proton of dppa and/or the carbonyl ligands of the iron centre, whereas the latter may be due to absence of reaction (SnR_4) or to deprotonation of the amino function by RLi or RMgX rapidly followed by adventitious reprotonation.

In the presence of a base like NEt_3 or DBU, *N*-deprotonation of **1b** occurred under mild conditions (below −30 °C) and chemical trapping of the transient bimetallic amide complex **C** by addition of a large excess of MeI gave the *N*-methyl derivative [$(OC)_3$Fe{μ-Si$(OMe)_2$(OMe)}(μ-dppaMe)PdCl] **9** (Scheme 4, Table 1). However, in the absence of alkyl halide,

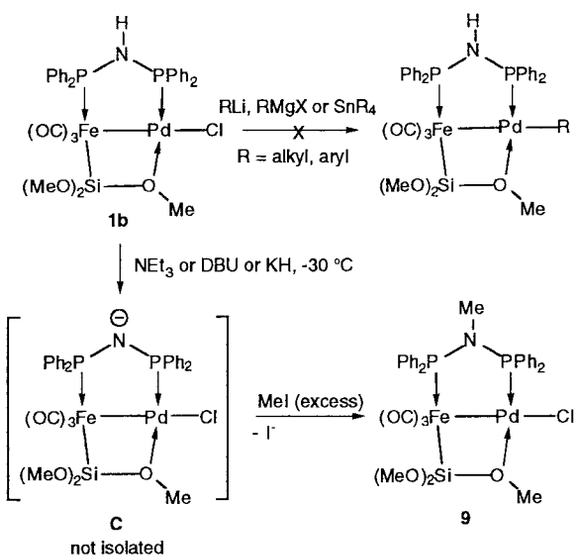

Scheme 4

reprotonation to **1b** was observed. The *N*-substitution could not be extended to other alkyl or functional groups, as recently reported for heterometallic clusters containing dppa.[18] Like in **1b**, the –Si$(OMe)_3$ group in **9** adopts a μ-η^2-Si–O coordination mode. A broad signal at δ 3.72 was observed for the methoxy protons in the room temperature ^1H NMR spectrum which again indicated a hemilabile behaviour of this ligand. Coalescence was reached at 271 K, giving a $\Delta G^{\ddagger} = 55.62 \pm 0.7$ kJ mol^{-1},[15] which is similar to that determined for **1b** (*vide supra*). Two signals at δ 3.66 and 3.82 in a 1 : 2 ratio are observed below the coalescence temperature.

Since clean formation of a Pd–C bond could not be achieved with **1b** owing to the occurence of side reactions, we used mononuclear Pd derivatives containing a Pd–C bond as precursors for the synthesis of the desired dppa-bridged Fe–Pd heterobimetallic complexes. This approach, shown in Scheme 5, was successful and complexes [$(OC)_3$-Fe{μ-Si$(OMe)_2$(OMe)}(μ-dppa)PdMe] **3b**, [$(OC)_3$-Fe{μ-Si$(OMe)_2$(OMe)}(μ-dppa)PdPh] **5b** and [$(OC)_3${$(MeO)_3$-Si}Fe(μ-dppa)Pd(η^3-allyl)] **8b** were obtained by reaction of the carbonylmetallate **2b** with [PdCl(Me)(COD)], [PdI(Ph)-(TMEDA)] (TMEDA = $Me_2NCH_2CH_2NMe_2$) and [Pd(η^3-allyl)(μ-Cl)]$_2$, respectively (Scheme 5, Table 1). In **8b** the 16 electron configuration of the Pd center is achieved by the η^3 coordination mode of the allyl ligand which explains the

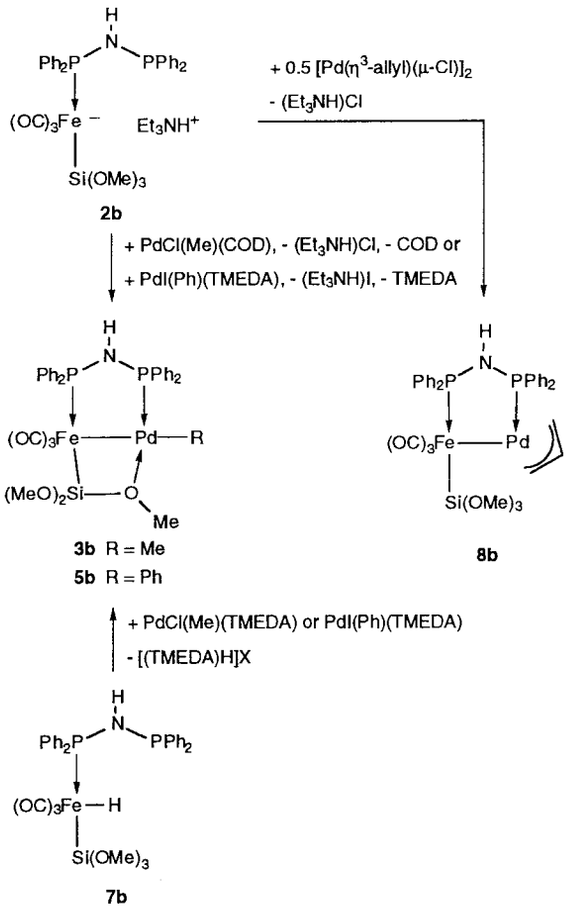

Scheme 5

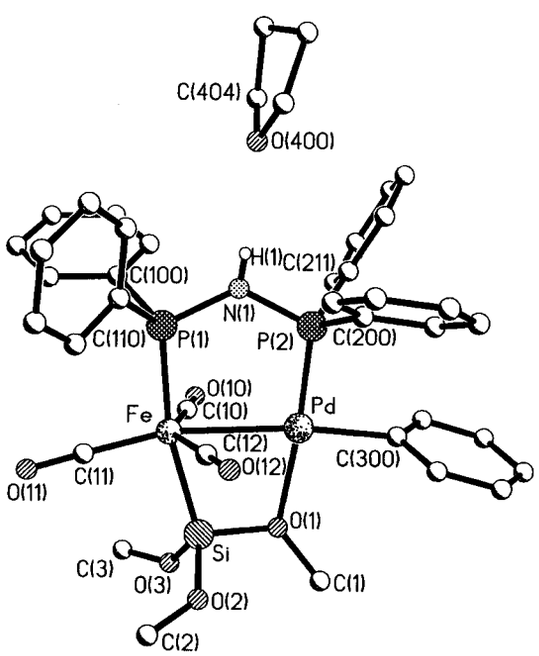

Fig. 3 ORTEP view of the structure of the complex **5b**·THF together with the atomic numbering scheme. The ellipsoids for the atoms are drawn at the 30% probability level.

absence of a μ-η^2-SiO→Pd bridging interaction, reflected in the large ^{2+3}J(PP) value of 116 Hz (Table 2).

Contrary to **3b** and **8b**, the aryl complex **5b** was obtained in low yield (<30%) and decomposition products such as [Fe(CO)$_3$(dppa-*P,P′*)] were observed. However, when [PdI(Ph)(TMEDA)] was reacted with the hydrido complex **7b**, complex **5b** was selectively formed and isolated in 65% yield. Improved yield and selectivity were also observed when **3b** was prepared following this approach (Scheme 5). The presence of [(TMEDA)H]X indicated that formation of the metal–metal bond resulted from a dehydrohalogenation reaction induced by the release of TMEDA. The methyl (**3a**) and phenyl (**5a**) dppm analogues of **3b** and **5b** were obtained similarly. Recall that **5a** could not be prepared by reaction of **1a** with arylating reagents (*vide supra*).

Table 5 Selected bond lengths (Å) and angles (°) for [(OC)$_3$Fe{μ-Si(OMe)$_2$(OMe)}(μ-dppa)PdPh]·THF (**5b**·THF)

Pd–Fe	2.654(1)	Si–O(2)	1.638(5)
Pd–O(1)	2.170(4)	Si–O(3)	1.626(5)
Pd–P(2)	2.179(1)	O(1)–C(1)	1.439(6)
Pd–C(300)	2.054(5)	O(2)–C(2)	1.304(8)
Fe–C(10)	1.772(6)	O(3)–C(3)	1.293(8)
Fe–C(11)	1.754(5)	Fe–P(1)	2.1965(14)
Fe–C(12)	1.767(5)	P(1)–C(100)	1.833(5)
C(10)–O(10)	1.162(6)	P(1)–C(110)	1.829(4)
C(11)–O(11)	1.163(6)	P(2)–C(200)	1.806(5)
C(12)–O(12)	1.164(6)	P(2)–C(210)	1.820(5)
Fe–Si	2.273(2)	N(1)–P(1)	1.689(4)
Si–O(1)	1.665(4)	N(1)–P(2)	1.678(4)
C(300)–Pd–O(1)	93.8(2)	C(12)–Fe–Si	84.4(2)
C(300)–Pd–P(2)	91.25(14)	P(1)–Fe–Si	168.51(6)
O(1)–Pd–P(2)	174.23(11)	C(10)–Fe–Pd	70.5(2)
C(300)–Pd–Fe	173.54(14)	C(11)–Fe–Pd	166.0(2)
O(1)–Pd–Fe	80.19(10)	C(12)–Fe–Pd	73.4(2)
P(2)–Pd–Fe	94.62(4)	P(1)–Fe–Pd	94.44(4)
C(300)–Pd–Si	126.75(14)	Si–Fe–Pd	74.08(5)
O(1)–Pd–Si	33.18(11)	O(1)–Si–Fe	104.15(14)
P(2)–Pd–Si	141.42(5)	O(2)–Si–Fe	118.9(2)
Fe–Pd–Si	47.12(4)	O(3)–Si–Fe	120.5(2)
C(10)–Fe–C(11)	107.7(2)	P(1)–N(1)–P(2)	126.5(3)
C(10)–Fe–C(12)	143.9(2)	Si–O(1)–Pd	101.3(2)
C(11)–Fe–C(12)	107.3(2)	N(1)–P(1)–Fe	111.7(2)
C(10)–Fe–P(1)	90.8(2)	N(1)–P(2)–Pd	112.2(2)
C(11)–Fe–P(1)	99.5(2)	O(10)–C(10)–Fe	176.8(5)
C(12)–Fe–P(1)	92.3(2)	O(11)–C(11)–Fe	179.0(5)
C(10)–Fe–Si	85.5(2)	O(12)–C(12)–Fe	176.5(5)
C(11)–Fe–Si	92.0(2)		

The solid-state structure of **5b**·THF was confirmed by an X-ray diffraction study. A view is shown in Fig. 3 and selected interatomic distances and angles are given in Table 5. The coordination geometries at the metal centres, square-planar at Pd and distorted octahedral at Fe, and the structural features resemble those found in **1b**. Compared to the latter, the more elongated Fe–Pd bond, 2.654(1) Å, of **5b**·THF becomes similar to that found in the dppm complex [(OC)$_3$Fe{μ-Si(OMe)$_2$(OMe)}(μ-dppm)Pd(SnPh$_3$)], 2.6655(5) Å.[13] As a result, the P(1)–N–P(2) angle is more obtuse in **5b**·THF, 126.5(3)°, than in **1b**, 121.8(12)°. The Pd–O(1) bond distance in **5b**·THF, 2.170(4) Å, is comparable to the corresponding one in **1b**, 2.178(19) Å. As in **1b**, the presence of a O(1)→Pd interaction leads to an elongation of the Si–O(1) bond, 1.665(4) Å, by comparison with the other Si–O bonds, 1.638(5) and 1.626(5) Å. The P(1)–Fe–Si angle, 168.51(6)°, is more acute than in **1b**, showing a slightly more distorted octahedral geometry at the iron centre. The phenyl ring attached to Pd is almost orthogonal to the mean palladium coordination plane (C(301)–C(300)–Pd–P(2) = 101.5°). In the crystals of **5b**·THF a molecule of tetrahydrofuran was found forming a hydrogen bridge with the amine H atom in the ligand with an O · · · H distance of 2.210 Å.

Reactivity studies

CO migratory insertion. When a slow stream of CO was passed through a CH_2Cl_2 solution of **3a** or **3b**, the acyl complexes **10a** and **10b** were formed quantitatively. Both compounds were isolated and could be stored for prolonged periods

of time without any observable de-insertion of CO. A $CDCl_3$ solution of **10a** stored at 253 K for 4 weeks contained only *ca.* 10% of **1a** as decomposition product. It appears that in the case of **3b** the lower electron donor properties of dppa, compared to dppm, enhance the rate of CO insertion, since only 30 min were required for complete conversion to **10b** against *ca.* 60 min for that of **3a** to **10a.** The probable mechanism of this reaction is pictured in Scheme 6. Although the proposed intermediate **D**

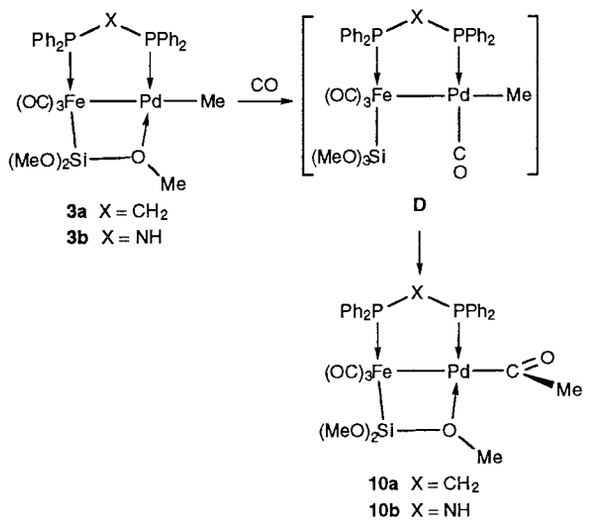

Scheme 6

was not detected by spectroscopic methods, its transient formation appears reasonable and its platinum analogue has been characterized by IR and ^{31}P NMR techniques.[8a]

The IR spectrum of **10a** showed a CO stretch of medium intensity at 1678 cm^{-1} for the acyl group, in addition to the three carbonyl vibrations at 1958, 1893 and 1864 cm^{-1} (Table 1). In the ^1H NMR spectrum (298 K, $CDCl_3$) the methoxy groups gave rise to a narrow singlet at δ 3.71, whereas a doublet at δ 1.82 was ascribed to the methyl protons of the acyl group ($^4J(PH)$ = 1.2 Hz). In the $^{13}C\{^1H\}$ NMR spectrum, the carbon atoms of the acyl group were found at δ 35.7 (Me, doublet, $^3J(PC)$ = 33 Hz) and δ 238.5 (C=O). The $Fe(CO)_3$ carbon atoms gave two doublets at δ 215.1 and 213.4 in a 2:1 ratio and a very broad "hump" at δ 52.3 was observed for the methoxy groups, due to slow rotation on the ^{13}C NMR time scale of the $-Si(OMe)_3$ ligand about the Fe–Si axis. No CO insertion was observed under similar conditions when a solution of **6a** was purged with CO. This is consistent with the absence in this complex of a fourth, labile coordination site on Pd, as in **3a**. It also indicates that carbonylation of **3a**,**b** occurs *via* an intermediate of type **D** rather than through a pentacoordinated intermediate that would have been also available in the case of **6a**.

A more complex reaction occurred when CO was bubbled through a solution of the benzyl derivative **4a** in THF (eqn. (2)). IR and $^{31}P\{^1H\}$ NMR monitoring indicated slow formation of the acyl complex $[(OC)_3Fe\{\mu\text{-}Si(OMe)_2(OMe)\}(\mu\text{-dppm})Pd\{C(O)CH_2Ph\}]$ **11a** (Table 1). The insertion rate was lower than in the case of **3a**, since after 3 h *ca.* 60% of **4a** was still present. This observation should be related to the reversibility of this carbonylation reaction since we observed that when a solution of **11a** was placed under reduced pressure, complete CO de-insertion from the acyl ligand regenerated **4a**. The acyl complex **11a** could hence only be characterized in solution by its AX pattern in the $^{31}P\{^1H\}$ NMR spectrum centered at δ 63.4 (P(Fe)) and 25.5 (P(Pd)) with a $^{2+3}J(PP)$ coupling of 56 Hz and the appearance of a broad ν(CO) band at 1678 cm^{-1}. This reaction was further complicated by the slow transformation of the acyl complex **11a**. Thus, after prolonged purging of a THF

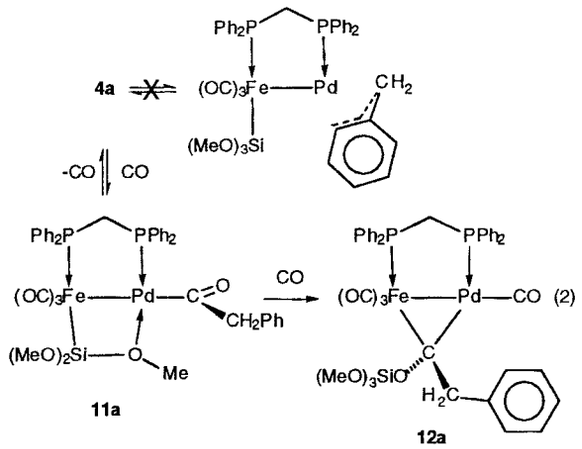

or CH_2Cl_2 solution with CO, the μ-siloxycarbene complex $[(OC)_3Fe\{\mu\text{-}C(CH_2Ph)OSi(OMe)_3\}(\mu\text{-dppm})Pd(CO)]$ **12a** was formed and unambiguously identified *in situ* by comparison of its spectroscopic data with those of the related complex $[(OC)_3Fe\{\mu\text{-}C(Me)OSi(OSiMe_3)_3\}(\mu\text{-dppm})Pd(CO)]$ (Table 6).[19a] After 7 h reaction time, the $^{31}P\{^1H\}$ NMR spectrum revealed the presence of **11a** and **12a** in a 1:9 ratio. This new complex is stable in THF for several hours under CO atmosphere, but decomposes during attempts at purification. Its IR spectrum exhibits three ν(CO) vibrations of the iron carbonyls at 2004 (m), 1948 (s) and 1925 (m) cm^{-1} and a band of medium intensity at 2032 cm^{-1} due to the Pd-bound carbonyl ligand. The large $^{2+3}J(PP)$ coupling of 137 Hz in the $^{31}P\{^1H\}$ NMR spectrum is also characteristic for this type of μ-siloxycarbene complexes.[7,19]

The proposed reaction mechanism for the formation of **12a**, shown in Scheme 7, is based on that previously

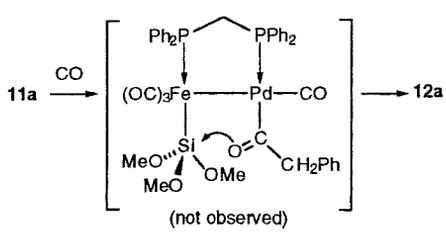

Scheme 7

established for the first examples of phosphine- or CO-induced migration of the siloxane unit in $[(OC)_3Fe\{\mu\text{-}Si(OSiMe_3)_2(OSiMe_3)\}(\mu\text{-dppm})PdMe]$ to yield such μ-siloxycarbene heterometallic complexes.[19a] Labeling experiments with ^{13}CO showed that the bridging carbene ligand originated from the acyl group. This reaction was quantitative within 5 min (without the formation of any detectable acyl intermediate) owing to the more electropositive character of the central Si atom of the $Si(OSiMe_3)$ ligand compared to $Si(OMe)_3$, which facilitates formation of the new Si–O bond. At present, we have no satisfactory explanation for the differing behaviour between the methyl and the benzyl ligands. It is well known that electron-withdrawing substituents on the α-carbon generally stabilize a metal–carbon bond and render migratory insertion reactions more difficult. Note that Anderson *et al.* have recently studied CO insertion into the Pd–Me bond of [PdCl(Me)(COD)], but observed decomposition on attempts to insert CO into $[PdCl(CH_2C_6H_4)(COD)]$.[20a] We found no spectroscopic evidence for an equilibrium between the benzyl complex **4a** and a conceivable η^3-benzyl isomer (eqn. (2)) that could have been related to the facile decarbonylation of **11a**. Such a situation was recently described by Lin and Yamamoto who observed that rapid decarbonylation

Table 6 $^{31}P\{^{1}H\}$ NMR (ppm, Hz) and IR data (cm^{-1}) of the μ-siloxycarbene complexes

Complex	δP_{Fe}	$\delta P_{Pd}{}^{a}$	$\delta P_{Pd}{}^{b}$	$^{2+3}J(PP^{a})$, $^{2}J(P^{a}P^{b})$	$\nu(CO)^{d}$
12a	62.0 (d)	13.9 (d)	—	137[c]	2032m, 2004m, 1948s, 1925m
13a	68.5 (d)	15.6 (dd)	8.8 (d)	135, 7[e]	1974m, 1904vs, 1895(sh)
14a	65.4 (dd)	14.9 (dd)	18.6 (t)	131, 4[e]	1980m, 1915vs, 1898s (sh)
14b	104.7 (d)	67.7 (dd)	18.1 (d)	150, 8[e]	1990m, 1923vs
15a	66.8	15.6	141.1	[e,f]	1984m, 1916vs

[a] P atom from the dppm or dppa ligand; [b] P atom from the monodentate ligand; [c] in THF–$CDCl_3$; [d] in CH_2Cl_2; [e] in $CDCl_3$; [f] $^{2+3}J(PP) = 135$, $^{2}J(PP) = 9$, $^{3+4}J(PP) = 6$ Hz.

Table 7 Correlation between ligand cone angle and pK_a for the PR_3-induced silyl migration

Complex	Cone angle/°	pK_a	Ligand
13a	132	8.69	PEt_3
14a	145	2.73	PPh_3
14b	145	2.73	PPh_3
15a	100.7	2.60	$P(OMe)_3$

of the stable phenylacetyl complex *trans*-[Pd{C(=O)CH_2-C_6H_4}Cl(PPh_3)$_2$] was induced by halide abstraction and yielded the cationic η^3-benzylpalladium complex [Pd(η^3-$CH_2C_6H_4$)-(PPh_3)$_2$][PF_6].[20b]

A silyl migration reaction also took place when **10a** was reacted with an equimolar amount of PEt_3. This led within 20 min to the quantitative formation of the μ-siloxycarbene complex [(OC)$_3$Fe{μ-C(Me)OSi(OMe)$_3$}(μ-dppm)Pd(PEt_3)] **13a** (Scheme 8, Table 6).

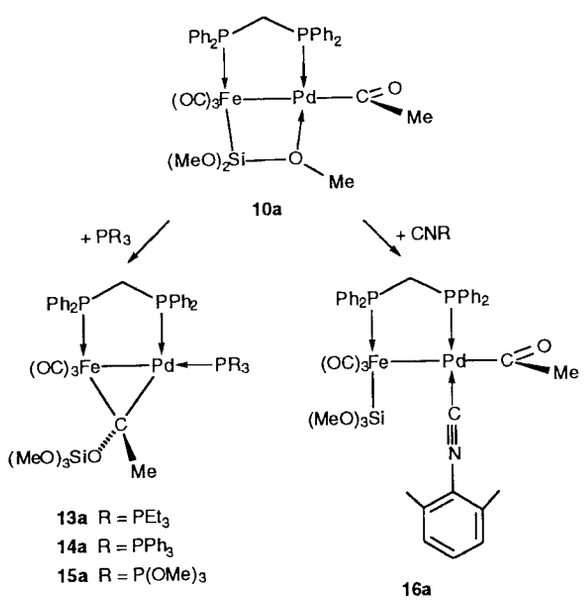

Scheme 8

As noted for the phosphine-induced rearrangement of the corresponding Fe–Pt acyl complexes leading to the μ-siloxycarbene complexes [(OC)$_3$Fe{μ-C(Me)OSi(OMe)$_3$}(μ-dppm)Pt(PR_3)],[19b] the basicity of the PR_3 ligand appears to play a more important role than its cone angle on the rate of this interesting rearrangement. This appears very clearly from Table 7.

IR monitoring of the reaction with PPh_3 revealed completion within *ca.* 1 h (disappearance of the acyl stretch at 1678 cm^{-1}), whereas in the case of $P(OMe)_3$ more than 2 h were needed, even in the presence of two equivalents of phosphite. Compared to their Fe–Pt counterparts, the stability of **13a**–**15a** in solution is markedly reduced, so that suitable crystals for an X-ray diffraction study could not be obtained. The proposed formulation of **13a**–**15a** could however unambiguously be confirmed by elemental analysis and spectroscopic data in the case of **13a** and **14a**, the more labile derivative **15a** was only characterized in solution (Table 6). The $^{13}C\{^{1}H\}$ NMR spectrum of **13a** recorded at 253 K contains a doublet of doublets ($^{2}J(PC) = 14$ and 77 Hz), diagnostic for a bridging carbene ligand, and three distinct doublets at δ 218.2, 219.2 and 220.6 for the carbonyl ligands. The $^{31}P\{^{1}H\}$ NMR spectrum consists of three resonances: the iron-bound phosphorus gives rise to a doublet at δ 68.5 with a $^{2+3}J(PP)$ coupling of 135 Hz. The resonance at δ 15.6 for the dppm phosphorus on Pd shows a further *cis*-coupling of 7 Hz with the PEt_3 ligand, which resonates at δ 8.8.

For comparison, reaction of **10b** with PPh_3 was carried out in CH_2Cl_2. Formation of the bridging siloxycarbene complex [(OC)$_3$Fe{μ-C(Me)OSi(OMe)$_3$}(μ-dppa)Pd(PPh_3)] **14b** was observed, but the reaction took 5 h even in the presence of 2 equivalents of PPh_3. This may be explained by the weaker electron donating properties of dppa compared to dppm which results in a lowering of the electron density on the acyl oxygen and therefore to a decreased propensity for Si–O(acyl) coupling and siloxycarbene rearrangement (Scheme 9). Complex **14b** was

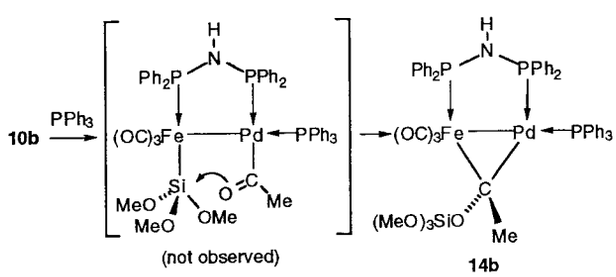

Scheme 9

obtained as a red powder, which is labile in chlorinated solvents. The spectroscopic data and the FAB^+ spectrum are in full agreement with the proposed structure (see Experimental section).

Addition of 2,6-xylyl isocyanide to **10a** instantaneously opened the dative O→Pd bond and the isocyanide adduct **16a** could be isolated (Scheme 8, Table 1). Even after 12 h in solution neither isocyanide insertion into the Pd–acyl bond nor a silyl migration reaction occurred. The $^{31}P\{^{1}H\}$ NMR spectrum recorded at 298 K contains a broad "hump" at δ 18.9 for the Pd-bound dppm-phosphorus, whereas the Fe-bound phosphorus gave rise to a sharp doublet centered at δ 66.0 with a $^{2+3}J(PP)$ coupling of 87 Hz. Progressive cooling of the solution induced a sharpening of the high field signal, which was finally resolved as a distinct doublet at 243 K. These observations could be explained by a partial, reversible dissociation of the isocyanide ligand.

Conclusion

In order to investigate further the insertion chemistry into the metal–carbon bond of heterobimetallic complexes, we have prepared diphosphine-bridged Fe–Pd methyl, benzyl, phenyl

and allyl complexes. It is interesting to contrast the reactivity of the hydride *mer*-[HFe{Si(OMe)$_3$}(CO)$_3$(dppa-*P*)] **7b** with [PdCl(Me)(COD)], which gives the chloro complex [(OC)$_3$-Fe{μ-Si(OMe)$_2$(OMe)}(μ-dppa)PdCl] **1b**, and with [PdX(R)-(TMEDA)] (X = Cl, R = Me; X = I, R = Ph), which afford the corresponding Fe–Pd–R hydrocarbyl complexes [(OC)$_3$-Fe{μ-Si(OMe)$_2$(OMe)}(μ-dppa)PdMe] **3b** or [(OC)$_3$-Fe{μ-Si(OMe)$_2$(OMe)}(μ-dppa)PdPh] **5b**, respectively. The different mechanism is due to the release in the latter case of the basic ligand TMEDA which deprotonates **7b**. CO insertion was observed under mild conditions in the complexes that contain a stabilizing but labile μ-η^2-SiO→Pd bridging interaction between the two metals. Opening of this dative interaction readily provides a coordination site for an entering substrate. For comparison, this interaction is lacking in complex [(OC)$_3${(MeO)$_3$Si}Fe(μ-dppm)Pd(8-mq)] **6a** and is replaced by a stable Pd–C–C–C–N chelate which does not lead to CO insertion under similar conditions. The reaction of CO with the benzyl complex [(OC)$_3$Fe{μ-Si(OMe)$_2$(OMe)}(μ-dppm)Pd-CH$_2$(Ph)] **4a** was reversible and more complex since the resulting acyl product [(OC)$_3$Fe{μ-Si(OMe)$_2$(OMe)}(μ-dppm)Pd-{C(O)CH$_2$Ph}] **11a** rearranged into the μ-siloxycarbene complex [(OC)$_3$Fe{μ-C(CH$_2$Ph)OSi(OMe)$_3$}(μ-dppm)Pd(CO)] **12a**. Reaction of the acetyl complex [(OC)$_3$-Fe{μ-Si(OMe)$_2$(OMe)}(μ-dppa)Pd{C(O)Me}] **10a** with PR$_3$ also resulted in silyl migration from iron to carbon and formation of similar μ-siloxycarbene complexes. In contrast, reaction with 2,6-xylyl isocyanide opened the μ-η^2-SiO→Pd bridge to give the stable complex [(OC)$_3${(MeO)$_3$Si}Fe(μ-dppm)Pd-(CN-2,6-xylyl){C(O)Me}] **16a**. Comparisons could be made between related dppm and dppa complexes and between complexes containing different R groups.

Experimental

All reactions were performed using Schlenk tube techniques under an atmosphere of purified nitrogen. Solvents were freshly distilled under nitrogen from the usual drying agent prior to use. Nitrogen was passed through BASF R3-11 catalyst and molecular sieve columns to remove residual oxygen and water. The ^{1}H, ^{31}P{^{1}H} and ^{13}C{^{1}H} NMR spectra were recorded at 300.13, 121.5 and 75 MHz respectively on a FT Bruker AC 300 instrument. The ^{29}Si-INEPT spectrum was recorded at 77.78 MHz (TMS standard) on a Bruker ACP 200 spectrometer. Infrared spectra were recorded in the 4000–400 cm^{-1} range on a IFS-66 Bruker FTIR spectrometer and in the 400–90 cm^{-1} range on a IFS-113 Bruker FTIR spectrometer. Mass spectra were measured on a Fisons ZAB-HF spectrometer (Université Louis Pasteur, R. Hubert). Elemental C, H and N analyses were performed by the Service de microanalyse (Université Louis Pasteur, Strasbourg).

Preparations

The ligands Ph$_2$PCH$_2$PPh$_2$ (dppm)[21] and Ph$_2$PNHPPh$_2$ (dppa)[22] and the complexes [PdCl(Me)(COD)],[23] [PdI(Ph)(T-MEDA)],[24] [Pd(8-mq)(μ-Cl)]$_2$,[25] [Pd(η^3-allyl)(μ-Cl)]$_2$[26] were prepared according to published procedures. Complexes K[Fe{Si(OMe$_3$)}(CO)$_3$(dppm-*P*)] **2a**, [HFe{Si(OMe$_3$)}(CO)$_3$-(dppm-*P*)] **7a** and [(OC)$_3$-Fe{μ-Si(OMe)$_2$(OMe)}(μ-dppm)Pd-Cl] **1a** were prepared as previously described.[11,27] An improved synthetic method is described below for [(OC)$_3$-Fe{μ-Si(OMe)$_2$OMe}(μ-dppa)PdCl] **1b**.[14]

[PdCl(Me)(TMEDA)]. A mixture of [PdCl(Me)(COD)] (0.610 g, 2.30 mmol) and TMEDA (0.35 mL, 2.30 mmol) in CH$_2$Cl$_2$ was stirred for 2 h. The volatiles were then removed under reduced pressure. The residue was washed with pentane and dried under reduced pressure. The desired product was obtained as a white powder. ^{1}H NMR (CDC1$_3$): δ 0.50 (3 H, s, PdCH$_3$), 2.50 (2 H, m, CH$_2$), 2.56 (6 H, s, NCH$_3$), 2.65 (6 H, s, NCH$_3$), 2.70 (2 H, m, CH$_2$). These data are in accordance with those given in the literature.[28]

[(OC)$_3$Fe{μ-Si(OMe)$_2$OMe}(μ-dppa)PdCl] 1b. To a solution of **7b** (see below) (0.510 g, 0.78 mmol) in CH$_2$Cl$_2$ (20 mL) at 273 K was added solid [Pd(η^3-allyl)(μ-Cl)]$_2$ (0.142 g, 0.39 mmol) or [PdCl(Me)(COD)] (0.206 g, 0.78 mmol). After it had been stirred at ambient temperature for 1 h, the solution was filtered through a pad of silica and Celite. The solvent was then removed under reduced pressure and **1b** was obtained as a yellow powder (0.492 g, 80% yield) (Found: C 45.48; H 4.07; N 1.80%. C$_{30}$H$_{30}$ClFeNO$_6$P$_2$PdSi requires C 45.71; H 3.84; N 1.78%); ν_{max}/cm^{-1} (Pd–Cl) 290m (polyethylene); ^{1}H NMR (CD$_2$Cl$_2$, 298 K): δ 3.70 [br, 9 H, Si(OMe)$_3$], 4.38 (br, 1 H, NH), 7.28–7.85 (m, 20 H, aromatics); ^{1}H NMR (CD$_2$Cl$_2$, 243 K): δ 3.49 [s, 3 H, Si(μ-OMe)Pd], 3.62 [s, 6 H, Si(OMe)$_2$], 4.50 (br, 1 H, NH), 7.28–7.85 (m, 20 H, aromatics).

[(OC)$_3$Fe{μ-Si(OMe)$_2$(OMe)}(μ-dppm)PdMe] 3a. *Method A*. Solid [PdCl(Me)(COD)] (0.264 g, 1.0 mmol) was added to a solution of K[Fe{Si(OMe$_3$)}(CO)$_3$(dppm-*P*)] **2a** (0.685 g, 1.0 mmol) in THF (25 mL) cooled to 273 K. Upon warming to ambient temperature, the solution turned dark green. It was then filtered through a Celite pad and concentrated to *ca*. 5 mL. After addition of hexane and stirring at 248 K, a green yellow solid was precipitated which was sufficiently pure for further reactions (NMR control) (0.574 g, 75% yield). An analytically pure sample of **3a** was obtained by extraction with warm Et$_2$O and subsequent evaporation of the solvent under reduced pressure. The desired complex was obtained as a bright yellow solid.

Method B. To a solution of [PdCl(Me)(TMEDA)] (0.080 g, 0.326 mmol) in toluene was added [HFe{Si(OMe$_3$)}-(CO)$_3$(dppm-*P*)] **7a** (0.212 g, 0.327 mmol). After the solution had been stirred for 4 h, it was filtered and the volatiles were evaporated under reduced pressure. The residue was then washed with pentane, dried under reduced pressure and **3a** was obtained as a bright yellow powder (0.180 g, 72% yield) (Found: C 50.19; H 4.36%. C$_{32}$H$_{34}$FeO$_6$P$_2$PdSi requires C 50.14; H 4.47%); ^{1}H NMR (benzene-d_6, 298 K): δ 0.82 (s, 3 H, PdMe), 3.49 [t, 2 H, PCH$_2$P, ^2J(PH) 10.1 Hz], 3.91 [s, br, 9 H, Si(OMe)$_3$], 6.92–7.65 (m, 20 H, aromatics); ^{13}C{^{1}H} NMR (CDCl$_3$, 298 K): δ 215.9 (d, 2 FeCO, ^2J(PC) 18 Hz), 213.4 (br, 1 FeCO), 123.5–146.2 (m, aromatics), 50.7 (s, br, SiOCH$_3$), 47.3 [dd, PCH$_2$P, ^1J(PC) 30 and 20 Hz], 15.7 (s, PdCH$_3$); ^{29}Si-INEPT (CDCl$_3$, 298 K): δ 17.6 (dd, ^2J(PSi) 32 Hz, ^3J(PSi) 5 Hz).

[(OC)$_3$Fe{μ-Si(OMe)$_2$(OMe)}(μ-dppa)PdMe] 3b. A few drops of NEt$_3$ and solid [PdCl(Me)(COD)] (1.33 g, 5.04 mmol) were added to a solution of **7b** (3.77 g, 5.04 mmol) in CH$_2$Cl$_2$ (15 mL) at 253 K. After being stirred at room temperature for 15 min, the solution turned green. It was then filtered. Addition of hexane caused precipitation of **3b** as a yellow powder which was collected by decantation and dried under reduced pressure (2.94 g, 76% yield) (Found: C 48.75; H 4.35; N 1.85%. C$_{31}$H$_{33}$FeO$_6$-NP$_2$PdSi requires C 48.49; H 4.33; N 1.82%); ^{1}H NMR (acetone-d_6, 298 K): δ −0.66 (s, 3 H, PdMe), 3.71 [s, 9 H, Si(OMe)$_3$], 3.98 [t, 1 H, NH, ^2J(PH) 5.2 Hz], 7.26–7.68 (m, aromatics).

[(OC)$_3$Fe{μ-Si(OMe)$_2$(OMe)}(μ-dppm)Pd(CH$_2$Ph)] 4a. To a stirred solution of **1a** (0.787 g, 1.0 mmol) in THF (15 mL) at 253 K was added 0.6 mL of a 2 M solution of benzyl magnesium chloride in THF (commercial from Aldrich). Upon warming to ambient temperature, the colour changed from dark red to orange brown. After addition of a few drops of MeOH to quench excess (PhCH$_2$)MgCl, the volatiles were removed under reduced pressure and the residue was washed with 5 mL of pentane. Complex **4a** was then obtained after extraction with warm diethyl ether (3 × 40 mL) and elimination of the solvent under reduced pressure (0.573 g, 68% yield). An analytically pure sample was obtained by recrystallization from toluene–hexane as orange-brown microcrystals (Found: C 54.30; H 4.59%. $C_{38}H_{38}FeO_6P_2PdSi$ requires C 54.14; H 4.54%); ^{1}H NMR ($CDCl_3$, 298 K): δ 2.77 (s, 2 H, PdCH$_2$), 3.76 [s, 9 H, Si(OMe)$_3$], 3.65 [dd, 2 H, PCH$_2$P, ^2J(PH) 9.7 and 12.0 Hz], 6.77–7.53 (m, 25 H, aromatics); ^{13}C{^{1}H} NMR ($CDCl_3$, 298 K): δ 215.9 [d, 2 FeCO, ^2J(PC) 18 Hz], 213.0 (br, 1 FeCO), 123.5–146.2 (m, phenyl), 50.8 (s, SiOCH$_3$), 47.6 [dd, PCP, ^1J(PC) 30 and 20 Hz], 41.5 [d, PdCH$_2$, ^2J(PC) 6 Hz].

[(OC)$_3$Fe{μ-Si(OMe)$_2$(OMe)}(μ-dppm)PdPh] 5a. *Method A*. To a stirred solution of [PdI(Ph)(TMEDA)] (0.045 g, 0.106 mmol) in toluene at 243 K was added solid [HFe{Si(OMe$_3$)}(CO)$_3$(dppm-*P*)] **7a** (0.070 g, 0.108 mmol). Upon warming to ambient temperature the solution turned red. After filtration, the volatiles were removed under reduced pressure and the residue was washed with pentane. Complex **5a** was obtained as a brown solid by extraction with Et$_2$O (0.034 g, 39% yield).

Method B. A large excess of KH was added at ambient temperature to a stirred solution of [HFe{Si(OMe$_3$)}(CO)$_3$(dppm-*P*)] **7a** (0.130 g, 0.201 mmol) in THF. This resulted in a vigorous gas evolution (H$_2$). After it had stopped, the solution was filtered and added to a stirred solution of [PdI(Ph)(TMEDA)] (0.085 g, 0.200 mmol) in THF (20 mL) at 253 K. The solution was allowed to warm to room temperature and was filtered. The volatiles were then removed under reduced pressure. Complex **5a** was extracted with Et$_2$O (0.055 g, 33% yield) (Found: C 53.81; H 4.45%. $C_{37}H_{36}FeO_6P_2PdSi$ requires C 53.61; H 4.38%); ^{1}H NMR (acetone-d_6, 298 K): δ 3.78 [s, 9 H, Si(OMe)$_3$], 4.1 [dd, 2 H, CH$_2$, ^2J(PH) 10.1 and 11.7 Hz], 6.68–7.72 (m, 25 H, aromatics).

[(OC)$_3$Fe{μ-Si(OMe)$_2$(OMe)}(μ-dppa)PdPh] 5b. *Method A*. Solid [PdI(Ph)(TMEDA)] (0.470 g, 1.10 mmol) was added to a stirred solution of **7b** (see below) (0.710 g, 1.10 mmol) in toluene at 253 K. The solution was stirred for 30 min at ambient temperature and was filtered. Addition of pentane caused the precipitation of **5b** as a yellow powder. The solvent was then decanted and the residue dried under reduced pressure (0.593 g, 65% yield).

Method B. Solid [PdI(Ph)(TMEDA)] (0.500 g, 1.17 mmol) was added to a stirred solution of **2b** (0.876 g, 1.17 mmol) in THF at 253 K. The solution was stirred for 3 h at ambient temperature and the volatiles were evaporated under reduced pressure. Complex **5b** was extracted with Et$_2$O and addition of hexane induced the precipitation of a yellow powder which was collected by decantation and dried under reduced pressure (0.428 g, 30% yield) (Found: C 51.88; H 4.17; N 1.72%. $C_{36}H_{35}FeNO_6P_2PdSi$ requires C 52.10; H 4.25; N 1.69%); ^{1}H NMR (toluene-d_8, 298 K): δ 3.75 [br, s, 10 H, Si(OMe)$_3$ and NH], 6.7–7.5 (m, aromatics).

[(OC)$_3${(MeO)$_3$Si}Fe(μ-dppm)Pd(8-mq)] 6a. A solution of **2a** (0.685 g, 1.0 mmol) in THF (25 mL) was added to a stirred slurry of [Pd(8-mq)(μ-Cl)]$_2$ (0.285 g, 0.5 mmol) in THF (10 mL) at 253 K. After warming to ambient temperature, the yellow solution was filtered and hexane was added. Upon slow concentration under reduced pressure, **6a** precipitated as a yellow, air stable powder (0.872 g, 92% yield). Suitable crystals for X-ray diffraction were obtained by layering a CH_2Cl_2 solution with hexane (Found: C 53.11; H 4.12; N 1.28%. $C_{41}H_{39}FeNO_6P_2PdSi{\cdot}CH_2Cl_2$ requires C 53.21; H 4.36; N 1.48%); ^{1}H NMR ($CDCl_3$, 298 K): δ 2.93 [d, 2 H, PdCH$_2$, ^3J(PH) 4.2 Hz], 3.55 [s, 9 H, Si(OMe)$_3$], 3.83 [dd, 2 H, PCH$_2$P, ^2J(PH) 9.5 and 11.1 Hz], 7.11–9.96 (m, 26 H, aromatics).

***mer*-[HFe{Si(OMe)$_3$}(CO)$_3$(dppa-*P*)] 7b.** A magnetically stirred solution of [Fe(CO)$_5$] (1.6 mL, 12.17 mmol) and HSi(OMe)$_3$ (4.6 mL, 36.51 mmol) in hexane was irradiated for 4 h at 283 K using a mercury lamp (180 W, TQ 150, Hereaus). The solution was allowed to warm to room temperature and was added in two portions to a solution of dppa (4.00 g, 10.4 mmol) in toluene. After each addition, the CO evolved was removed under reduced pressure for 1 min. After keeping the mixture at 253 K for 12 h, the solution was filtered and the solvent was evaporated under reduced pressure to afford **7b** as a brown, air sensitive oil. ^{1}H NMR (CD_2Cl_2, 298 K): δ −9.2 [d, FeH, ^2J(PH) 23 Hz], 3.4 (br s, NH), 3.6 [s, 9 H, Si(OMe)$_3$], 7.00–7.91 (m, 20 H aromatics).

[(OC)$_3$Fe{Si(OMe)$_3$}(μ-dppa)Pd(η^3-C$_3$H$_5$)] 8b. To a stirred solution of **2b** (1.245 g, 1.66 mmol) at 253 K was added [Pd(η^3-allyl)(μ-Cl)]$_2$ (0.305 g, 0.83 mmol). The solution was allowed to warm to room temperature and was filtered. After concentration, addition of hexane caused the precipitation of **8b** as a yellow powder. After decantation, the residue was washed with pentane and dried under reduced pressure (1.08 g, 82% yield) (Found: C 49.40; H 3.92; N 1.84%. $C_{33}H_{35}FeNO_6P_2PdSi$ requires C 49.92; H 4.44; N 1.76%); ^{1}H NMR (acetone-d_6, 298 K): δ 2.56 (m, 2 H, allyl), 2.90 (br, 1 H, NH), 3.53 [s, 9 H, Si(OMe)$_3$], 3.77 (m, 1 H, allyl), 5.01 (m, 1 H, allyl), 5.45 (m, 1 H, allyl), 7.2–7.6 (m, 20 H, aromatics).

[(OC)$_3$Fe{μ-Si(OMe)$_2$(OMe)}(μ-dppaMe)PdCl] 9. Complex **1b** (0.120 g, 0.15 mmol) was treated with excess KH (*ca.* 0.030 g) in THF at 233 K. After gas evolution (H$_2$) had ceased, excess MeI (0.46 mL, 1.06 g, 7.5 mmol) was added. The solution was stirred for 2 h at ambient temperature and filtered. The volatiles were then evaporated under reduced pressure and **9** was obtained as a red powder, which was washed with cold Et$_2$O (10 mL, 273 K) and pentane (2 × 10 mL) (0.081 g, 68% yield) (Found: C 46.45; H 4.12; N 1.81%. $C_{31}H_{32}ClFeNO_6P_2PdSi$ requires C 46.41; H 4.02; N 1.75%); ν_{max}/cm^{-1} (Pd–Cl) 241m (polyethylene); ^{1}H NMR (CD_2Cl_2, 298 K): δ 2.26 [dd, 3 H, NMe, ^3J(PH) 6.5 and 8.6 Hz], 3.72 [br, 9 H, Si(OMe)$_3$], 7.10–7.89 (m, 20 H, aromatics); ^{1}H NMR (CD_2Cl_2, 253 K): δ 2.26 [dd, 3 H, NMe, ^3J(PH) 6.5 and 8.6 Hz], 3.66 [s, 3 H, Si(μ-OMe)-Pd], 3.82 [s, 6 H, Si(OMe)$_2$], 7.10–7.89 (m, 20 H, aromatics).

[(OC)$_3$Fe{μ-Si(OMe)$_2$(OMe)}(μ-dppm)Pd{C(O)Me}] 10a. Carbon monoxide was bubbled through a solution of **3a** (0.766 g, 1.0 mmol) in CH_2Cl_2 (20 mL) at ambient temperature for 1 h. After the solution was stirred for a further 30 min under an atmosphere of CO, the red-brown solution was concentrated to *ca.* 5 mL. After layering with Et$_2$O, orange microcrystals of **10a** were formed after 2 days at 278 K (0.548 g, 69% yield) (Found: C 49.61; H 4.23%. $C_{33}H_{34}FeO_7P_2PdSi$ requires C 49.86; H 4.31%); ^{1}H NMR ($CDCl_3$, 298 K): δ 1.82 [d, 3 H, C(O)CH$_3$, ^4J(PH) 1.2 Hz], 3.66 [dd, 2 H, PCH$_2$P, ^2J(PH) 9.9 and 11.4 Hz], 3.71 [s, 9 H, Si(OMe)$_3$)], 7.15–7.79 (m, 20 H, aromatics); ^{13}C{^{1}H} NMR ($CDCl_3$, 298 K): δ 238.5 [d, *C*(=O)CH$_3$, ^2J(PC) 19 Hz], 215.1 [d, 2 FeCO, ^2J(PC) 19 Hz], 213.4 [d, 1 FeCO, ^2J(PC) 12 Hz], 136.5–128.2 (m, aromatics), 52.3 [vbr, Si(OCH$_3$)$_3$], 45.1 [dd, PCP, ^1J(PC) 20 and 31 Hz], 35.7 [d, C(O)CH$_3$, ^3J(PC) 33 Hz].

Table 8 Summary of crystal data, data collection and structure analysis

	1b	**5b**·THF	**6a**·hexane
Empirical formula	$C_{30}H_{30}ClFeNO_6P_2PdSi$	$C_{40}H_{43}FeNO_7P_2PdSi$	$C_{47}H_{53}FeNO_6P_2PdSi$
Formula weight	788.30	902.03	980.21
Crystal size/mm	0.60 × 0.30 × 0.30	0.24 × 0.24 × 0.14	0.18 × 0.24 × 0.23
Crystal system	Trigonal	Orthorhombic	Monoclinic
Space group	$R\bar{3}$	*Pbca*	$P2_1/n$
a/Å	25.113(2)	19.6245(3)	11.562(2)
b/Å	25.113(2)	13.9778(1)	21.028(3)
c/Å	25.113(2)	29.5777(6)	18.837(3)
α/°	118.39(2)		
β/°	118.39(2)		97.00(2)
γ/°	118.39(2)		
Volume 10^6/Å^3	5176(18)	8113.4(2)	4546(1)
D_{calc}/g cm^{-3}	1.519	1.477	1.432
Z	6	8	4
μ(Mo-Kα)/mm^{-1}	0.3955	0.958	0.8504
2θ range/°	6–52	2.76–50.0	6–50
Reflections collected	21577	43249	8470
Independent reflections	6781 [*R*(int) = 0.035]	7150 [*R*(int) = 0.065]	2910 [*R*(int) = 0.033]
Data/parameters	6781/395	6879/473	3029/535
Final *R* indices	*R1* = 0.032	*R1* = 0.051	*R* = 0.055
[$I > 2\sigma(I)$]	*wR2* = 0.127	*wR2* = 0.101	R_W = 0.075
Largest diff. peak/e Å^{-3}	1.02	0.462	1.08
Weighting scheme	$w = 1/[\sigma^2(F_o^2) + (0.0314P)^2 + 30.07P]$	$w = 1/[\sigma^2(F_o^2) + (0.0343P)^2 + 12.76P]$	$w = 1/[\sigma^2 F_o + 0.004\ F_o^2]$

[(OC)$_3$Fe{μ-Si(OMe)$_2$(OMe)}(μ-dppa)Pd{C(O)Me}] 10b. Carbon monoxide was bubbled through a solution of **3b** (0.767 g, 1 mmol) in CH_2Cl_2 (10 mL) at 293 K. After 30 min, the volatiles were removed under reduced pressure and the residue was washed with pentane affording **10b** as an orange powder (0.740 g, 92% yield) (Found: C, 48.69; H, 4.15; N, 1.51%. $C_{32}H_{33}FeNO_7P_2PdSi$ requires C 48.29; H 4.18; N 1.76%); ^{1}H NMR ($CDCl_3$, 298 K): δ 1.91 [s, 3 H, C(O)CH_3], 3.68 [s, 9 H, Si(OMe)$_3$)], 4.02 (br, 1 H, NH), 7.21–7.80 (m, 20 H, aromatics).

Complexes 11a and 12a. These were characterized *in situ*, see main text.

Carbene complexes [(OC)$_3$Fe{μ-C(Me)OSi(OMe)$_3$}(μ-dppx)Pd(PR$_3$)] 13a, 14a,b and 15a. *General procedure*. To a solution of **10a** or **10b** (0.2 mmol) in CH_2Cl_2 (5 mL) was added excess PR_3 (see below). After the reaction mixture was stirred at ambient temperature, the volatiles were removed under reduced pressure, the residue was triturated with hexane (3 mL) and then dried to give the desired product as a powder.

*Complex **13a** (dppx = dppm; PR$_3$ = PEt$_3$).* Reaction conditions: PEt_3 (0.22 mmol), reaction time: 30 min (0.173 g, 95% yield) (Found: C, 51.52; H, 5.63%; $C_{39}H_{49}FeO_7P_3PdSi$ requires C 51.30; H 5.41%); ^{1}H NMR ($CDCl_3$, 298 K): δ 0.89 (m, 9 H, CH_2CH_3), 1.20 (m, 3 H, PCH^AH^B), 1.44 (m, 3 H, PCH^AH^B), 2.84 [dt, 3 H, CH_3, ^4J(PH) 12.1 and 4.1 Hz], 3.38 [t, 2 H, PCH_2P, ^2J(PH) 9.6 Hz], 3.66 (s, 9 H, OCH_3), 7.04–7.85 (m, 20 H, aromatics); ^{13}C{^{1}H} NMR ($CDCl_3$, 253 K): δ 220.6 [d, FeCO, ^2J(PC) 25 Hz], 219.2 [d, FeCO, ^2J(PC) 6 Hz], 218.2 [d, FeCO, ^2J(PC) 25 Hz], 199.4 [dd, μ-C, ^2J(PC) 14 and 77 Hz], 51.6 (s, OCH_3), 45.0 (s, C-CH_3), 42.4 (m, PCP), 16.8 [dd, PCH_2CH_3, ^1J(PC) 18 Hz, ^3J(PC) 4 Hz], 8.4 [t, PCH_2CH_3, ^2J(PC) = ^4J(PC) 12 Hz].

*Complex **14a** (dppx = dppm; PR$_3$ = PPh$_3$).* Reaction conditions: PPh_3 (0.22 mmol), reaction time: 60 min (0.178 g, 85% yield) (Found: C 58.24; H 4.69%. $C_{51}H_{49}FeO_7P_3PdSi$ requires C 57.94; H 4.67%); ^{1}H NMR ($CDCl_3$, 298 K): δ 2.29 [dt, 3 H, CH_3, ^4J(PH) 10.2 and 2.9 Hz], 3.51 (s, 9 H, OCH_3), 3.30–3.65 [m, partially obscured by the Si(OMe)$_3$ resonance, 2 H, PCH_2P], 6.85–7.85 (m, 35 H, aromatics); ^{13}C{^{1}H} NMR ($CDCl_3$, 253 K): δ 220.6 [d, FeCO, ^2J(PC) 25 Hz], 219.2 [d, FeCO, ^2J(PC) 6 Hz], 218.2 [d, FeCO, ^2J(PC) 25 Hz], 199.4 [dd, μ-C, ^2J(PC) 14 and 77 Hz], 51.6 (s, OCH_3), 45.0 (s, C-CH_3), 42.4 (m, PCP), 16.8 [dd, PCH_2CH_3, ^1J(PC) 18, ^3J(PC) 4 Hz], 8.4 [t, PCH_2CH_3, ^2J(PC) = ^4J(PC) 12 Hz].

*Complex **14b** (dppx = dppa; PR$_3$ = PPh$_3$).* Reaction conditions: PPh_3 (0.4 mmol), reaction time: 4 h (0.109 g, 53% yield). A correct elemental analysis could not be obtained for this complex. ^{1}H NMR ($CDCl_3$, 298 K): δ 2.32 [dt, 3 H, CH_3, ^4J(PH) 12.9 and 4.6 Hz], 3.48 (s, 9 H, OCH_3), 4.26 (m, not resolved, 1 H, NH), 6.99–7.91 (m, 35 H, aromatics); mass spectrum (FAB$^+$, NBA matrix): 1056 (M^+, 3%), 973 ($M^+ - 3$ CO, 79%). The simulated isotopic distribution pattern was in agreement with the experimental spectrum.

*Complex **15a** (dppx = dppm; PR$_3$ = P(OMe)$_3$).* Reaction conditions: P(OMe)$_3$ (0.4 mmol), reaction time: 3 h. A correct elemental analysis could not be obtained for this complex. ^{1}H NMR ($CDCl_3$): δ 2.91 [ddd, 3 H, CH_3, ^4J(PH) 11.1, 5.2 and 3.5 Hz], 3.40 [d, 9 H, $POCH_3$, ^3J(PH) 13.0 Hz], 3.64 (s, 9 H, $SiOCH_3$), 3.35–3.70 [m, partially overlapped by the P(OMe)$_3$ and the Si(OMe)$_3$ resonance, 2 H, PCH_2P], 7.15–7.85 (m, 35 H, aromatics).

[(OC)$_3${(MeO)$_3$Si}Fe(μ-dppm)Pd(CN-2,6-xylyl){C(O)Me}] 16a. Xylyl isocyanide (0.0262 g, 0.2 mmol) was added to a solution of **10a** (0.159 g, 0.2 mmol) in CH_2Cl_2 (5 mL) at ambient temperature. After the brown-yellow solution was stirred for 10 min, it was concentrated under reduced pressure to 2 mL. After addition of hexane, **16a** precipitated as a yellow powder, which was dried under reduced pressure (0.167 g, 90% yield) (Found: C, 54.11; H, 4.32; N 1.38%. $C_{42}H_{43}FeNeO_7P_2PdSi$ requires C, 54.47; H, 4.68; N 1.51%); ^{1}H NMR ($CDCl_3$, 248 K): δ 1.84 [s, 3 H, C(=O)CH_3], 2.47 (s, 6 H, xylyl-CH_3), 3.51 (s, 9 H, Si(OMe)$_3$), 3.69 [t, 2 H, PCH_2P, ^2J(PH) 7.1 Hz], 7.05–7.71 (m, 23 H, aromatics).

X-Ray structure determinations of [(OC)$_3${(MeO)$_3$Si}-Fe(μ-dppm)Pd(8-mq) 6a·hexane, [(OC)$_3$-Fe{μ-Si(OMe)$_2$OMe}(μ-dppa)PdCl] 1b and [(OC)$_3$-Fe{μ-Si(OMe)$_2$(OMe)}(μ-dppa)PdPh] 5b·THF

Crystal data and experimental details are given in Table 8. The X-ray data were collected at room temperature on a Siemens SMART CCD area detector diffractometer (**5b**·THF) with a crystal-to-detector distance of 3.85 cm, on an Enraf Nonius

CAD4 (**6a**·hexane) and on a Philips PW 1100 diffractometer (**1b**) using graphite monochromated Mo-K_α radiation ($\lambda = 0.71073$ Å). The collected data were corrected for Lorentz and polarization effects. An empirical absorption correction with the program SADABS was applied to **5b**·THF.[29] The structures were solved by Patterson methods using SHELXS86[30] (**1b** or **6a**·hexane) or direct methods (**5b**·THF) using SIR92[31] and refined by the full-matrix least-squares based on F_o^2 (SHELXL93, SHELX96[32] for **1b** and **5b**·THF) or F_o (**6a**·hexane).[33] In the crystals of **6a** disordered molecules of hexane were also found. All non-hydrogen atoms were refined anisotropically (excepting the carbon atoms of the phenyl groups in **6a**·hexane which were refined isotropically) and the hydrogens were included in idealized positions. All calculations for **6a**·hexane and **1b** were carried out on the DIGITAL ALPHA255 of the Centro di Studio per la Strutturistica Diffrattometrica of C.N.R., Parma.

CCDC reference number 186/1690.

See http://www.rsc.org/suppdata/dt/1999/4175/ for crystallographic files in .cif format.

Acknowledgements

We are grateful to the Ministère de l'Enseignement Supérieur, de la Recherche et de la Technologie and the CNRS for financial support and to Johnson Matthey PLC for a generous loan of $PdCl_2$.

References

1 (*a*) J. P. Collman, L. S. Hegedus, J. R. Norton and R. G. Finke, *Principles and Applications of Organotransition Metal Chemistry*, University Science Books, Mill Valley, CA, 1987; (*b*) G. W. Parshall and S. Ittel, *Homogeneous Catalysis*, Wiley, New York, 1992; (*c*) A. Yamamoto, *J. Chem. Soc.*, *Dalton Trans.*, 1999, 1027.

2 (*a*) E. Drent, *Pure Appl. Chem.*, 1990, **62**, 661; (*b*) J. Tsuji, *Palladium Reagents and Catalysis*, Wiley, Chichester, 1995.

3 (*a*) R. M. Moriarty, W. R. Epa and A. K. Awasthi, *J. Am. Chem. Soc.*, 1991, **113**, 6315; (*b*) A. de Meijere and F. E. Meyer, *Angew. Chem.*, *Int. Ed. Engl.*, 1994, **33**, 2379; (*c*) W. Cabri and I. Candiani, *Acc. Chem. Res.*, 1995, **28**, 2; (*d*) J. M. Brown and K. K. Hii, *Angew. Chem.*, *Int. Ed. Engl.*, 1996, **35**, 657; (*e*) W. A. Herrmann, C. Brossmer, C.-P. Reisinger, T. H. Riermeier, K. Öfele and M. Beller, *Chem. Eur. J.*, 1997, **3**, 1357; (*f*) K. K. Hii, T. D. W. Claridge and J. M. Brown, *Angew. Chem.*, *Int. Ed. Engl.*, 1997, **36**, 984; (*g*) G. Trabesinger, A. Albinati, N. Feiken, R. W. Kunz, P. S. Pregosin and M. Tschoerner, *J. Am. Chem. Soc.*, 1997, **119**, 6315; (*h*) C. P. Mehnert and J. Y. Ying, *Chem. Commun.*, 1997, **22**, 2215; (*i*) K. Albert, P. Gisdakis and N. Rösch, *Organometallics*, 1998, **17**, 1608.

4 (*a*) H. Alper, J. B. Woell, B. Despeyroux and D. J. H. Smith, *J. Chem. Soc.*, *Chem. Commun.*, 1983, **21**, 1270; (*b*) S. P. Gupte and R. V. Chaudhari, *J. Mol. Catal.*, 1986, **34**, 241; (*c*) S. I. Murahashi, Y. Mitsue and K. Ike, *J. Chem. Soc.*, *Chem. Commun.*, 1987, **2**, 125; (*d*) G. P. Chiusoli, M. Costa, S. Reverberi, G. Salerno and M. G. Terenghi, *Gazz. Chim. Ital.*, 1987, **117**, 695; (*e*) P. Leconte, F. Metz, A. Mortreux, J. A. Osborn, F. Paul, F. Petit and A. Pillot, *J. Chem. Soc.*, *Chem. Commun.*, 1990, **22**, 1616; (*f*) J. Tsuji and T. Mandai, *J. Organomet. Chem.*, 1993, **451**, 15; (*g*) P. Wehman, G. C. Dol, E. R. Moorman, P. C. J. Kamer, P. W. N. M. van Leeuwen, J. Fraanje and K. Goubitz, *Organometallics*, 1994, **13**, 4856; (*h*) Y. S. Lin and A. Yamamoto, *Organometallics*, 1998, **17**, 3466.

5 (*a*) M. Brookhart, F. C. Rix, J. M. DeSimone and J. C. Barborak, *J. Am. Chem. Soc.*, 1992, **114**, 5894; (*b*) A. Sen, *Acc. Chem. Res.*, 1993, **26**, 303; (*c*) F. C. Rix, M. Brookhart and P. S. White, *J. Am. Chem. Soc.*, 1996, **118**, 4746; (*d*) W. Keim and H. Maas, *J. Organomet. Chem.*, 1996, **514**, 271; (*e*) E. Drent and P. H. M. Budzelaar, *Chem. Rev.*, 1996, **96**, 663; (*f*) G. J. P. Britovsek, K. J. Cavell, M. J. Green, F. Gerhards, B. W. Skelton and A. H. White, *J. Organomet. Chem.*, 1997, **533**, 201; (*g*) K. Nozaki and T. Hiyama, *J. Organomet. Chem.*, 1999, **576**, 248.

6 (*a*) S. Mecking, L. K. Johnson, L. Wang and M. Brookhart, *J. Am. Chem. Soc.*, 1998, **120**, 888 and references cited therein; (*b*) G. J. P. Britovsek, V. C. Gibson and D. F. Wass, *Angew. Chem.*, *Int. Ed.*, 1999, **38**, 429 and references cited therein.

7 P. Braunstein, M. Knorr and C. Stern, *Coord. Chem. Rev.*, 1998, **178**–**180**, 903 and references cited therein.

8 (*a*) P. Braunstein, M. Knorr and T. Stährfeldt, *J. Chem. Soc.*, *Chem. Commun.*, 1994, **17**, 1913; (*b*) P. Braunstein, M. Knorr, J. Cossy, P. Vogel and C. Strohmann, *New. J. Chem.*, in the press; (*c*) M. Knorr, C. Strohmann and P. Braunstein, *Organometallics*, 1996, **15**, 5653.

9 (*a*) P. Braunstein, X. Morise and J. Blin, *J. Chem. Soc.*, *Chem. Commun.*, 1995, **14**, 1455; (*b*) P. Braunstein and X. Morise, *Organometallics*, 1998, **17**, 540; (*c*) P. Braunstein, J. Durand, X. Morise, A. Tiripicchio and F. Ugozzoli, *Organometallics*, in the press.

10 (*a*) L. W. Arndt, B. T. Bancroft, M. Y. Darensbourg, C. P. Janzen, C. M. Kim, J. Reibenspies, K. E. Varner and K. A. Youngdahl, *Organometallics*, 1988, **7**, 1302; (*b*) A. Fukuoka, S. Fukagawa, M. Hirano and S. Komiya, *Chem. Lett.*, 1997, 377; (*c*) A. Fukuoka, T. Sadashima, T. Sugiura, X. Wu, Y. Mizuho and S. Komiya, *J. Organonomet. Chem.*, 1994, **473**, 139.

11 P. Braunstein, M. Knorr, A. Tiripicchio and M. Tiripicchio-Camellini, *Angew. Chem.*, *Int. Ed. Engl.*, 1989, **28**, 1361.

12 (*a*) P. Braunstein, T. Faure, M. Knorr, T. Stährfeldt, A. DeCian and J. Fischer, *Gazz. Chim. Ital.*, 1995, **125**, 35; (*b*) M. Knorr and P. Braunstein, *Bull. Soc. Chim. Fr.*, 1992, **129**, 663.

13 P. Braunstein, M. Knorr, H. Piana and U. Schubert, *Organometallics*, 1991, **10**, 828.

14 J. Blin, P. Braunstein, J. Fischer, G. Kickelbick, M. Knorr, X. Morise and T. Wirth, *J. Chem. Soc.*, *Dalton Trans.*, 1999, 2159.

15 $\Delta G^\ddagger$ values for exchange processes observed *via* NMR spectroscopy were calculated by using the Eyring equation, see: H. Günther, *NMR-Spektroskopie*, Georg Thieme Verlag, Stuttgart, 1983, Ch. 8.

16 L. S. Benner and A. L. Balch, *J. Am. Chem. Soc.*, 1978, **100**, 6099.

17 R. Uson, J. Fornies, M. Tomas, J. M. Casas and C. Fortuno, *Polyhedron*, 1989, **8**, 2209.

18 (*a*) I. Bachert, P. Braunstein and R. Hasselbring, *New J. Chem.*, 1996, **20**, 993; (*b*) I. Bachert, I. Bartussek, P. Braunstein, E. Guillon, J. Rosé and G. Kickelbick, *J. Organomet. Chem.*, 1999, **580**, 257; (*c*) M. Knorr and C. Strohmann, *Eur. J. Inorg. Chem.*, 1998, **1**, 495.

19 (*a*) M. Knorr, P. Braunstein, A. Tiripicchio and F. Ugozzoli, *Organometallics*, 1995, **14**, 4910; (*b*) M. Knorr, P. Braunstein, A. DeCian and J. Fischer, *Organometallics*, 1995, **14**, 1302.

20 (*a*) R. A. Stockland, G. K. Anderson, N. P. Rath, J. Braddock-Wilking and J. C. Ellegood, *Can. J. Chem.*, 1996, **74**, 1990; (*b*) Y.-S. Lin and A. Yamamoto, *Organometallics*, 1998, **17**, 3466.

21 K. Sommer, *Z. Anorg. Chem.*, 1970, **376**, 37.

22 H. Nöth and L. Meinl, *Z. Anorg. Allg. Chem.*, 1967, **349**, 223.

23 F. T. Lapido and G. K. Anderson, *Organometallics*, 1994, **13**, 303.

24 B. A. Markies, A. J. Canty, W. de Graaf, J. Boersma, M. D. Janseen, M. P. Hogerheide, W. J. J. Smeets, A. L. Spek and G. van Koten, *J. Organomet. Chem.*, 1994, **482**, 191.

25 A. J. Deeming and I. P. Rothwell, *J. Organomet. Chem.*, 1981, **205**, 107.

26 M. Sakakibara, Y. Takahashi, S. Sakai and Y. Ishii, *Chem. Commun.*, 1969, 396.

27 P. Braunstein, M. Knorr, U. Schubert, M. Lanfranchi and A. Tiripicchio, *J. Chem. Soc.*, *Dalton Trans.*, 1991, 1507.

28 W. de Graaf, J. Boersma, W. J. J. Smeets, A. L. Spek and G. van Koten, *Organometallics*, 1989, **8**, 2907.

29 SADABS, Program for Siemens area detector absorption correction, G. M. Sheldrick, Universität Göttingen, 1996.

30 G. M. Sheldrick, SHELX86, Program for Crystal Structure Solutions, Universität Göttingen, 1986.

31 A. Altomare, M. C. Burla, M. Camalli, G. Cascarano, C. Giacovazzo, A. Guagliardi and G. Polidori, SIR92, *J. Appl. Crystallogr.*, 1994, **27**, 435.

32 G. M. Sheldrick, SHELX93 and SHELX96, Program for the refinement of crystal structures, Universität Göttingen, 1993 and 1996.

33 G. M. Sheldrick, SHELX76, Program for Crystal Structure Determinations, University of Cambridge, 1976.

34 C. K. Johnson, ORTEP, Report ORNL-5138, Oak Ridge National Laboratory, Oak Ridge, TN, 1976.

Paper 9/07425B